Department of Biomedical Sciences

(Head: Univ.-Prof. Mathias Müller)

University of Veterinary Medicine Vienna

Institute for Animal Breeding and Genetics

(Head: Univ.-Prof. Mathias Müller)

Genetics of Ultraviolet Radiation and Reactive Oxygen in the Origin of Melanoma

MASTER THESIS

for obtaining the degree

Master of Science (MSC.)

of the University of Veterinary Medicine Vienna

submitted by

Silvia WALLISCH

Vienna, December 2011

This MASTER THESIS was conducted at Yale School of Medicine

External Supervisor: Prof. Douglas Brash, PHD (Department of Therapeutic Radiology, Yale School of Medicine)

Internal Supervisor: Prof. Dr. Marina Karaghiosoff (Institute for Animal Breedings and Genetics, University of Veterinary Medicine, Austria)

Reviewer:

List of abbreviations

8-Oxo-2-deoxyguanosine	8-oxo-dG
α-MSH	α- melanocyte stimulating hormone
ACTH	Adrenocorticotropic hormone
ASP	Agouti signaling protein
CDHI	Cadherin-1
CPD	Cis-syn cyclobutane pyrimidine dimers
dbcAMP	Dibutyryl cyclic adenosine monophosphate
DCT	Copachrome tautomerase
DHI	5,6 dihydroxyindole
DHICA	5,6 dihydroxyindole-2-carboxylic acid
FADH	Flavin adenine dinucleotide hydrogen
FBS	Fetal Bovine Serum
GSTP1	Glutathione S-transferase Pi 1;
hFGF	Human basic fibroblast growth factor
IBMX	3-isobutyl-1-methylxanthine
LAMA3	Laminin alpha 3
LAMC2	Laminin gamma 2
MAPK	Mitogen activated protein kinase

MC1R	Melanocortin receptor 1
MITF	Master transcriptional regulator of pigmentation
MMPs	Matrix metalloprotease
NADH	Nicotinamide adenine dinucleotide hydrogen
PBS	Phosphate Buffered Saline
(6-4) PPs	Pyrimidine (6-4) pyrimidone photoproducts
SOD	Superoxide dismutase
TPA	12-O-tetradecanoylphorbol-13-acetate
TRP-1	Tyrosinase related protein
TYR	Tyrosinase
UV	Ultraviolet

TABLE OF CONTENTS

1 Introduction

1.1 Solar ultraviolet radiation (Solar UV)

The sun emits a broad spectrum of electromagnetic radiation including visible (400-700 nm), UV (200-400 nm), infrared (700-2000 nm) and small amounts of radio, microwave, X-ray and gamma ray bands. The region representing UV radiation is most closely related to skin damage and can be subdivided into UVA (320-400 nm), UVB (290-320) and UVC (200-290 nm). However, the contribution of UVC can be neglected due to its absorption by the earth's ozone layer.

1.2 The human skin

1.2.1 Histology of the skin

Human skin is a multi layered squamous epithelium and consists of two parts: the epidermis and the dermis. The main purpose of the epidermis is to function as a barrier against environmental influences and damaging agents such as fungi, bacteria and viruses, as well as UV. It consists of 4 layers, namely: Stratum corneum, Stratum granulosum, Stratum spinosum, and Stratum basale.

Stratum corneum is the outermost layer and is composed of corneocytes, which are mainly dead keratinocytes lacking nuclei and organelles. These cells form a barrier against infections and protect from dehydration. Stratum granulosum harbors granulocytes, which are keratinocytes from Stratum spinosum that contain keratohyalin and various proteins. Near the base of the epidermis lies a layer of germinative keratinocyte stem cells (Statum basale) capable of proliferation and differentiation (CLAYTON et al., 2007). Intermingled with these germinative skin stem cells are the melanocytes, cells specialized to produce the skin pigment melanin. Melanocytes derive from neural crest cells and during embryogenesis migrate as melanoblasts to the epidermis of the skin (HEARING et al. 2005)

The epidermis also comprises Langerhans cells, which are dendritic cells of the skin, able to present foreign antigen to cells of the immune system.

Below the epidermis lies the dermis, a layer composed of collagen, elastic and reticular fibers(which are composed of type III collagen) and harboring fibroblasts, macrophages and adipocytes. The dermis also has blood vessels, nerves and specialised organelles for touch and pressure.

1.2.2 Pigmentation

Pigmentation of the skin is managed by melanin, a biopolymer pigment, which is found not only in melanocytes but also in brain (ADLER, 1942), inner ear (WOLFF, 1931) and in the retina of the eye (FEENEY-BURNS, 1980). There are two types of melanin: pheomelanin (yellowish, reddish) and eumelanin (brownish, blackish). Both are synthesized in melanosomes and transported via dendrites to neighboring keratinocytes. In both melanocytes and keratinocytes, melanin accumulates as a supranuclear cap to absorb radiation (mostly UV and visible light). However, these supranuclear caps are mainly found in dark pigmented skin, and not in fair pigmented skin (KOBAYASHI et al., 1998). Studies on the photo-protective role of melanin shows that black epidermis allows only 7.4% UVB and 17.5% UVA to penetrate, while white skin allows 24% UVB and 55% UVA (HALDER and BRIDGEMAN-SHAN, 1995).

1.2.2.1 Synthesis of melanin

Melanin biosynthesis is a complex enzymatic pathway, summarized by SIMON et al. (2009) (Fig. 1). The enzyme tyrosinase oxidizes the amino acid tyrosine in two steps to dopa and then dopaquinone. After the addition of an aminogroup to dopaquinone, cyclodopa is produced. Cyclodopa is then rapidly oxidized to dopachrome, which is decarboxylated to DHI and DHICA. These two are tautomers and oxidize to form the polymer eumelanin. It is described that DHI oxidation occurs by redox exchange with

DQ, whereas the oxidation of DHICA requires the action of DHICa oxidase or tyrosinase.

The production of pheomelanin includes the addition of cysteine to dopaquinone, followed by redox exchange between cyclodopa and dopaquinone to generate cysteinyldopa-quinones and dopa. Further dehydration forms 1,4-Benzothiazine intermediates(namely BT, ODHBT and BZ). These molecules are then polymerized to form pheomelanin.

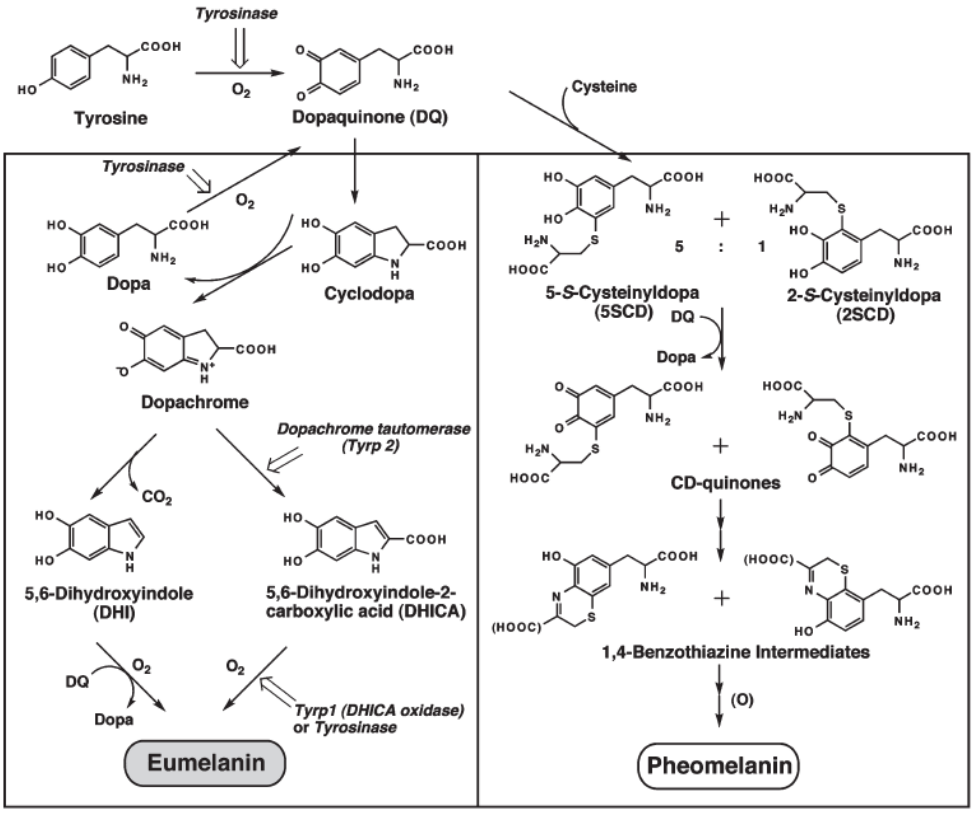

Fig. 1: Synthesis of eumelanin and pheomelanin (adapted from: SIMON et al., 2009).

1.2.2.2 Regulation of melanin synthesis

Melanocortin Receptor 1 (MC1R) plays a main role in the pigment phenotype. It is a G-protein coupled receptor that regulates the quantity and quality of melanin (REESE, 2000). The activity of MC1R is in turn regulated by the agonists α-MSH and ACTH and the antagonist ASP. Recent studies by HIDA et al. (2009) showed that ASP is also an agonist for pheomelanin production even in the absence of α-MSH. α-MSH and ACTH up-regulate the activity of MC1R, which leads to upregulation of cAMP and the production of eumelanin (dark skin color). In contrast, ASP leads to a down-regulation of MC1R eliciting the production of pheomelanin (fair skin color and red/blonde hair).

UV is the most prominent factor influencing pigmentation of the skin. As a direct effect of UV, especially UVA, the skin shows immediate pigment darkening which persists minutes to hours. This immediate response is not due to increased melanin synthesis but rather by oxidation and polymerization of existing melanin and the redistribution of melanosomes (YOUNG, 2006).

Delayed pigment darkening appears hours after exposure and lasts up to days and weeks. Here, exposure to UV leads to an increased expression of *MITF* in the melanocyte*. MITF* is a transcription factor that increases the transcription of the genes for its down-stream proteins Pmel17, MART-1, TYR, TRP1 and DCT (MIYAMURA et al., 2007). Moreover, UV stimulates the production of α-MSH and ACTH. Incident UV on keratinocytes stimulates the production of endothelin 1, which up-regulates the production of MC1R. Further, interleukin 1 is up-regulated leading to increased secreted levels of ACTH, α-MSH and endothelin 1. P53 in keratinocytes is also stimulated by UV, resulting in an increased expression of the *POMC* gene, which stimulates the secretion of ACTH and α- MSH.

1.2.3 Damage to the skin due to UV

1.2.3.1 Acute

UV radiation is able to penetrate the skin and cause damage on molecular and cellular levels. Therefore, it is responsible for a wide variety of different acute and chronic effects on the skin.

- Acute responses of human skin to UVR include skin and in some cases also eye photodamage, erythema, DNA photoproducts, immunosuppression, synthesis of vitamin D, and tanning.
- Chronic UVR effects include photoaging, photocarcinogenesis and mutation.

Erythema is an acute injury following excessive exposure to UV radiation. When the source of radiation is sunlight, the reaction is commonly referred to as ‘sunburn’. The observed redness results from an increased blood content of the skin by dilatation of the superficial blood vessels in the dermis. The minimal dose that is needed to cause reddening of the skin is called the minimal erythemal dose (MED). This particular dose is dependent on the skin pigmentation of the subject. For instance, a fair skinned person can sustain 148 J/m^2 UVR before developing erythema, whereas a dark pigmented person can receive a 5 fold higher dose (KAIDBEY et al., 1979). Two different forms of erythema dependent on incident UV type can be observed:

- UVB-induced erythema: occurs approximately 4 hr after exposure, peaks around 8 to 24 hr, and fades after one or two days. This phenomenon is mainly induced by cytokines such as IL-1, Il-10, IL-6, IL-8 which are upregulated after UVB exposure (CLYDESDALE, et al., 2001)
- UVA induced erythema: shows two components: i) Immediate erythema: occurs immediately and fades after 4 hours. ii) Delayed erythema: exhibits a similar time course as UVB. Here IL-10 and IL-12 are upregulated after UVA exposure leading to inflammation (CLYDESDALE, et al., 2001)

A prominent population of cells, called sunburn cells, is formed 24h post UV after extensive UV exposure. These cells derive from keratinocytes that undergo apoptosis, characterized by a shrunken nuclei and an eosinophilc cytoplasm (YOUNG, 1987). On the molecular level it was shown that this apoptosis is p53-dependent (ZIEGLER et al 1994) and these cells exhibit a decreased DNA repair activity.

1.2.3.2 Chronic

Chronic UV exposure is the major factor for aging of sun-exposed skin. This phenomenon is referred to as photoaging. In contrast, chronologic aging appears as a smooth and unblemished surface, but with a loss of elasticity. Photoaging, on the other hand shows a splotchy leathery appearance with deep wrinkles (KLIGMAN and LAVKER, 1988).

Several studies provided a molecular explanation for photoaging by showing that UV leads to an abnormal accumulation of elastic tissue in the dermis termed solar elastosis (THOMAS et al, 2010). Additionally, KLIGMAN et al (2008) investigated UV related changes in collagen metabolism and found that chronic UVA increased the cross linking of collagen in hairless mice thus making it almost insoluble to pepsin digestion (87% insoluble fraction in comparison to 16% in unirradiated controls). The observed thinning of the skin results due to UV's blocking of the growth factor receptor that regulates collagen synthesis (QUAN et al., 2004). Moreover, UV down-regulates type I and III procollagen, and induces Matrix metalloprotease 1 which degrades skin collagen (FISHER et al., 2002)

1.3 Reactive Oxygen Species (ROS)

1.3.1 Physiological generation

Molecular oxygen (O_2) is essential for aerobic organisms to produce energy in form of adenosinetriphosphate (ATP). It is generated by oxidation of sugars, resulting in CO_2 and H_2O. The constant production of ATP is crucial and therefore has to be guaranteed. Most ATP is produced in the respiratory chain on mitochondrial membranes. Here an electrochemical gradient is produced, which fuels an ATP-synthase to produce ATP. Electrons are donated from electron donors (such as NADH, FADH) to an electron acceptor (O_2). This process is known as oxidative phosphorylation. During this process highly reactive and only partially reduced oxygen species are produced, so called reactive oxygen species (ROS). These species include: Superoxide anion (O_2^-), and hydroxyl radicals ($OH^\bullet$). These molecules have an unpaired electron and are therefore highly reactive with other molecules. During a process called Fenton reaction Fe (III) or Cu (III) donates an electron to H_2O_2 generating hydroxyl radical ($OH^\bullet$). The Haber-Weiss reaction uses H_2O_2 and O_2^- to generate $OH^\bullet$ by using Fe(III) as an electron shuttle.

Besides the respiratory chain in mitochondria, the cytoplasm of hepatocytes, specifically, is another production site of ROS. Here specific enzymes, referred to as cytochrome P450 oxidases, metabolize lipids and steroidal hormones as well as toxic chemicals and drugs. During this metabolism, ROS are constantly produced.

Furthermore, phagocyic cells such as macrophages and neutrophils use ROS to destroy foreign pathogens in a process called a “respiratory burst” (DAHLGREN and KARLSSON, 1999)

1.3.2 Environmental generation

Evidence indicates that melanin acts as a double-edged sword, by being a photoprotector as well a photosensitizer (HILL et al., 1997). The biosynthesis of melanin generates H_2O_2 during the formation of o-quinones (MUNOZ-MUNOZ et al., 2009). Also, melanin exposed to UV generates superoxide by transferring an electron to oxygen (CHEDEKEL et al., 1978). Superoxide and H_2O_2 can, in the presence of free iron ions (FeIII), interact with each other and generate the most reactive ROS, the hydroxyl ion (McCORD, 1998). Hydroxyl ions are able to induce DNA single strand breaks (BALASUBRAMANIAN et al., 1998).

According to the type of melanin, Pheomelanin (yellowish, reddish) shows a greater ROS generating potential then eumelanin (brown and black) (CHEDEKEL et al., 1978). Moreover, cultivating melanocytes in tryosine containing media (results in an increased melanin production) yields in a 3 fold increase in UVA induced photosensitivity (WENCZEL et al.1998). BOSE et al (1989) found a UVA dependent increase in lipid peroxidation after irradiation, which contributes to DNA damage by ROS production. HILL and HILL (2000) demonstrated that UVA exposed cells with a higher melanin content showed more DNA damage then fairer pigmented cells and that an increased amount of pheomelanin photosensitizes DNA in fair pigmented cells.

1.3.3 Scavenging

The ROS production is a strictly regulated sensitive system. The mechanisms which underlie the ROS regulation involve the direct activation of kinases (Apoptosis signal-regulating kinase 1, Protein-Kinase C) and transcription factors for mainly AP1 (activation protein 1) and Nf-κB as well as the indirect modulation of cystein-rich proteins, especially glutathione and thioredoxin (ADLER et al., 1999)

The intracellular levels of ROS are regulated by various enzymes such as SOD, catalase, glutathione and peroxidase. In humans there are 3 forms of SOD:

- SOD I: localized in the cytoplasm, containing copper and zinc
- SOD II: localized in mitochondria, containing manganese
- SOD III: localized extracellularly, containing copper and zinc

SOD catalyzes the reaction from superoxide radicals to H_2O_2. The H_2O_2 causes together with Cu (III) (SAGRIPANTI and KRAEMER, 1989) or iron (III) (LOEB et al., 1988) single strand breaks and oxidizes DNA bases. To prevent this, the enzyme catalase, also localized in mitochondria, converts H_2O_2 into H_2O and O_2. Another way to eliminate H_2O_2 is the ascorbate-glutathione cycle as well as the glutathione peroxidase cycle. Other molecules involved in scavenging ROS include vitamins, such as vitamin C and E.

1.4 Mutagenesis

1.4.1 UVA mutagenesis

Recent studies report that not only UVB is relevant for the formation of photoproducts, but also UVA. ROCHETTE et al. (2003) found that CPDs in Chinese hamster ovary cells were also produced after exposure to UVA and that their predominant mutation sites were TTs rather than TC, CT or CC sites (57% versus 18, 11 and 14%, respectively). IKEHATA et al. 2009 found that UVA induces C to T base changes at dipyrimidine sites associated with CpG much more frequently than UVB. A study by PFEIFER et al. (2005) exposed mouse fibroblasts to UVA and UVB and found that the base exchange from G to T seems to be a signature mutation for UVA. In contrast to ROCHETTE et al. (2003), PFEIFFER et al (2005) were not able to find any CC to TT mutations in UVA exposed mouse fibroblasts.

Since, UVA is absorbed much less by DNA than UVB is, its mutagenic effect is related more to oxidative damage than to photoproduct formation. The prominent base formed by oxidative damage is 8-oxo-dG (ZHANG et al, 1997) (Fig. 2).

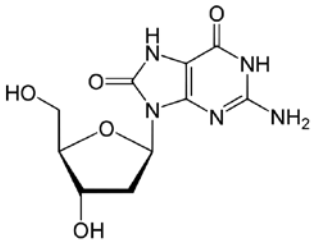

Fig. 2: Chemical structure of 8-oxo-dG (adapted from: ZHANG et al., 1997).

ZHANG et al. (1997) showed that the ratio of 8-oxo-dGuo to dimers increased nearly 1000-fold in both UVA-irradiated cells and DNA compared with those irradiated with UVB and UVC. Although the importance of UVB is widely known, the effects of UVA should not be neglected due to increased UVA exposure by using tanning studios and UVB-only protective sunscreens (URBACH, 1993).

1.4.2 UVB mutagenesis

SETLOW (1974) postulated that exposure to sunlight is the predominant cause for the development of melanoma and non melanoma skin cancers. UV generates various types of DNA damage such as DNA photoproducts and oxidative damage. Particularly, UVB can be absorbed directly by DNA, which leads to three major photoproducts: namely CPDs (LIPPKE et al., 1981) and (6-4) PPs (MITCHELL et al., 1986) and Dewar isomers (Fig. 3). In UV-irradiated DNA, the (6-4) TT photoproduct is formed much less frequently than the cis-syn TT dimer; the (6-4) lesion, however, is more mutagenic than the dimer The (6–4) photoproduct is formed much more frequently at TC and CC sites than at TT sites, and at the TC site, the (6–4) lesion is formed almost as frequently as a CPD (BRASH et al., 1987). COCK et al. (1992) irradiated *Drosophila melanogaster* cells and found that 31% of (6-4) PP lesions were repaired 4 hr post exposure to UVC. Another study conducted by CHANDRASEKHAR and VAN HOUTEN (2000) came to the same conclusion, showing that 42% of (6-4)PPs formed in *E.coli* cells were repaired

in the first hour post exposure to UVC. Supporting this data D'ERRICO et al. (2003) showed that approximately 50% of (6-4) PPs are repaired in both human keratinocytes and fibroblasts in the first 4 hours.

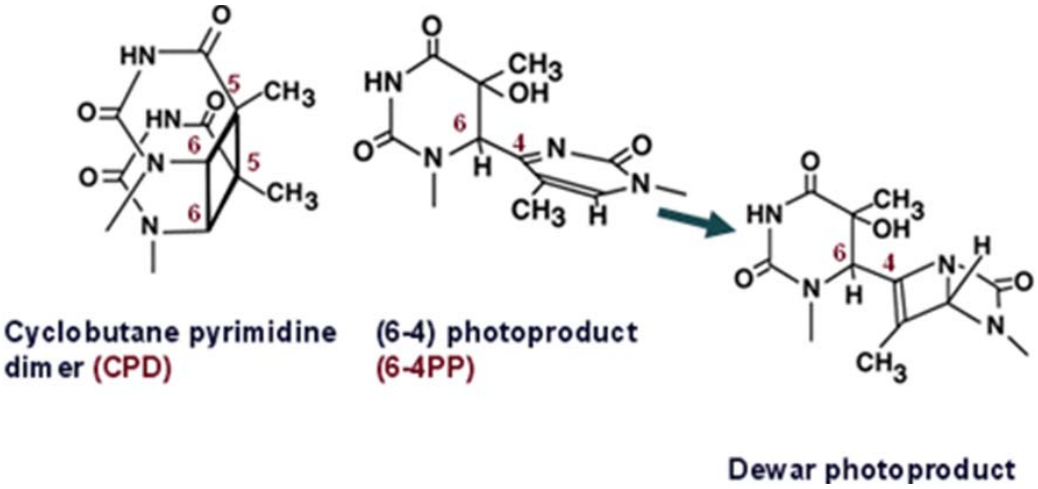

Fig. 3: Three major photoproducts produced by absorption of UV (adapted from http://www.cosmobio.co.jp)

BRASH et al. (1991) investigated squamous cell carcinomas and found that approximately 60% exhibited mutations in the tumor suppressor gene p53. Three of these tumors showed the presence of CC to TT double-base changes, which is a known UV signature mutation.

However, these lesions are mostly repaired by the nucleotide excision repair (NER). Once DNA damage occurs, the expression of p53 protein is upregulated and the damage is either repaired or if too severe cells are sent into apoptosis. Studies on Xeroderma pigmentosum (XP) patients (which lack DNA repair activity) show the importance of this mechanism in preventing skin cancer. In a study of XP patients, BRADFORD et al (2011) examined 106 XP patients and observed that 65% of the participants exhibited a 10,000 fold higher risk for developing non melanoma skin cancer and a 2000 fold increase for melanoma. LO et al (2005) concluded from their studies on NER-deficient XPA cells that the response to UV-induced 6-4 PP lesions is

to trigger apoptosis, whereas those of CPDs is to induce cell cycle arrest. Further, different studies support the predominant role of CPDs, because of its higher yield in production and slower removal, in contrast to 6-4 PPs.

YAMAGUCHI et al (2006) used the TUNEL assay to determine apoptotic cell level in different skin types and observed elevated 6-4 PP, CPD and p53 levels in fair skin after UV exposure, compared with dark skin. However, apoptotic cells showed an increased level in darker skin. They concluded that both a lower DNA damage level and higher removal of damaged cells in darker skin acts photoprotectively and contribute to the decreased skin cancer level in dark skinned people.

1.5 Melanoma

1.5.1 Epidemiology

Melanoma is a potentially lethal form of skin cancer that arises from malignant melanocytes. The number of patients diagnosed with melanomas is increasing every year and has been estimated as 3-7% in fair skinned Caucasians per year, which suggest a doubling in rates every 10-20 years (DIEPGEN and MAHLER, 2002). The Surveillance, Epidemiology, and End Results (SEER) registry of the United States estimated the age-adjusted incidence rate was 20.8 per 100,000 men and women per year. The median age of patients diagnosed with melanoma was 60 years with a median mortality at 68 years between 2004-2008. Survival is highly dependent on the stage at which it is diagnosed. If the lesion is localized at its primary site, there is a 98% survival chance. However, after the cancer has metastasized and formed distant clones the survival chance decreases to 15% (SEER, 2000). Potential melanoma precursors are atypical dysplastic nevi which are characterized by an intraepithelial melanocytic dysplasia. The WHO states dysplastic nevi as risk factors and potential precursors of melanoma (WHO, 2011). Another link is drawn between exposure to ultraviolet radiation (UVR) and melanoma formation.

1.5.2 Genes associated with melanoma formation

Different genes have been associated with melanoma genesis. One of them is *CDKN2A*. It encodes two tumor suppressor proteins: p14/ARF and p16(INK4A). Both of them have an indirect effect on p53, which is referred to as the “guardian of the genome”. P53 has an important role in cell cycle arrest, apoptosis and DNA repair. It has a short life due to ubiquitination by MDM2 (HDM) protein. However, if under stress (eg. hypoxia or DNA damage) p14/ARF binds to MDM2, therefore allowing p53 to escape degradation. Mutation in p14/ARF can lead to decreased production levels resulting in degradation of p53. Then p53 is not able to induce apoptosis or initiate DNA repair, which can lead to damage accumulation and mutations.

p16/INK4a functions together with the retinoblastoma (Rb) protein to induce G1 phase arrest during the cell cycle. P16 binds to a cyclin dependent kinase (CDK) to inhibit phosphorylation of Rb. Rb prevents the cell from replicating damaged DNA before it reaches the S-phase.

The MAP Kinase pathway, which is related to transcription and cell proliferation, is also involved in the formation of melanoma. A receptor tyrosine kinase (eg. KIT) phosphorylates RAS, a membrane bound protein with GTP activity. The activated RAS phosphorylates Map Kinase Kinase Kinase which leads to a chain reaction of phosphorylations, ending in MAP Kinase phosphorylating Cyclin D. Phosphorylated

Mutations in the *RAS* gene can be found in 13-25% of melanomas (CURTIN et al., 2005). The most common form is a replacement of glutamine with arginine at codon 61. BALL et al. (1994) examined 100 melanoma samples and found *RAS* mutations 2 to 3 fold more frequently in primary tumors form continuously exposed skin than tumors from intermittently or non-exposed skin sites.

BRAF another protooncogene is found at a high incidence in melanoma skin cancers (approximately 50%). In contrast to *NRAS* mutations *BRAF* mutations are most common in melanomas derived from non UV exposed areas (CURTIN et al. 2005). However, these mutation frequencys are even higher in non-malignant nevi (moles), where they can be found at a frequency of around 82% (POLLOCK et al., 2003). Most

prevalent is the mutation which introduces an amino acid substitution at valine 600. These mutations result in higher BRAF kinase activity which leads to an increased phosphorylation of Map Kinase Kinase.

CURTIN et al. (2006) investigated the somatic activation of *KIT* in melanomas with a low incidence of *BRAS* and *NRAF* mutations and found increased copy numbers in *KIT* in 39% of mucosal, 36% of acral, and 28% of melanomas on chronically UV damaged skin.

1.6 Methylation in cancer

DNA methylation is an important mechanism of gene regulation and allows genes to go from an active state to an inactive state. The term "methylation" refers to an addition of a methyl group (CH3) to either the 5th carbon in cytosine (resulting in 5-methylcytosine) or the 6th nitrogen of adenine (resulting in N6 methyl adenine) (Fig. 4).

a) **b)**

Fig. 4: The two prominent bases that are formed during methylation : **a)** 5-methylcytosine and **b)** N6 methyl adenine

DNA methylation is catalyzed by an enzyme called DNA methyltransferase. In mammals three types have been identified: DNMT 1, DNMT II and DNMT III. Two different forms have to be distinguished, active *de novo* methyltransferases (DNMT3a and DNMT3b) and maintainance metyltransferases that maintain existing methylation patterns (DNMT1). Most methylations occur at CpG sites. These dinucleotides occur at a frequency of 5 to 10 % in the human genome. However, there are areas with a higher

frequency of these CpG dinucleotides called CpG islands (around 60% GC with a ratio of CpG to GpC of at least 0.6) (BAYLIN et al., 1998). These CpG islands often lie within a gene or in close proximity. In the human genome, 80-90% of CpG sites are methylated whereas CpG islands are mostly unmethylated (ANTEQUERA and BIRD, 1993). Hypermethylation of CpG islands and hypomethylation of specific loci can be found in various cancers (DAS and SINGAL, 2004). The *BRCA1* gene was shown to be hypermethylated in breast cancer (DOBROVIC and SIMPFENDORFER, 1997), *p16* in lung and GIT BAuylincancer (HERMAN et al., 1995), p15 in squamous cell carcinoma (GARCIA et al., 2002) and GSTP1 (ESTELLER et al, 1998). Hypomethylation was also found in cancer, including *cMYC* and *hRAS* (FEINBERG, 1983). BROWN et al. (2004) reported that p16, p14 and CDH1 show hypermethlyation in squamous cell carcinoma. SATHYANARAYANA et al. (2007) investigated aberrant promoter methylation of 12 genes in basal cell carcinomas, squamous cell carcinomas and normal skin lesions and found hypermethylation in CDH1, LAMA3 and LAMC2. They also found significant hypermethylation in sun exposed areas, whereas sun protected areas exhibited little to no methylation. Recent studies by JONES and BAYLIN (2002) found the tumor suppressor gene *Von Hippel-Lindau (VHL)* was hypermethylated in renal cancer. They suggested that this loss of gene function is a contributor in developing cancer.

A study by LIM et al. (2008) provided evidence that ROS induces Snail in hepatocellcarcinoma, which induces E-cadherin promoter methylation leading to its down-regulation.

1.7 Aims of this study

Our hypothesis is that, in melanocytes, susceptibility to UV-induced skin cancer is mediated in part by direct absorption of UV by DNA, leading to the production of CPDS and failure to sequester ROS, both resulting in DNA damage (8-oxo-dG). These DNA damages can lead to mutations and epigenetic changes. There is evidence that the pigmentary system is an internal source of ROS (MUNOZ-MUNOZ et al., 2009). Moreover, UV irradiated Melanin shows increased ROS level (TAKEUCHI et al., 2004). The type of melanin, pheomelanin vs eumelanin and the amount of melanin in the cells play a crucial role in ROS production. Especially pheomelanin (in individuals with blonde and red hair) is shown to be photosensitizing by increasing the internal production of ROS after exposure to UV (WENCZL et al., 1998). High levels of ROS lead not only to stochastic DNA damage and rare mutation but also to epigenetic changes that silence tumor suppressor genes (BROWN et al., 2004). These epigenetic changes also silence ROS-scavenging genes, creating a “cancer-positive” feedback loop (KOGA et al., 2009). Because epigenetic changes, like mutations, are inherited through cell division by DNA methytransferases, they may chronicle the “history” of environmental UV-induced insults to form malignant lesions.

This thesis will gain data concerning the production of ROS and the resulting DNA damages (8-oxo-dG) due to photosensitization in melanocytes and fibroblasts after UV exposure. Another aim is to determine epigenetic changes in melanocytes associated with generation of ROS and find possible new target genes that are methylated by ROS production. Once optimal conditions are established, ROS production and methylation will be determined in albino melanocytes and melanocytes carrying the Mc1r (e/e) allele (typical for individuals with blonde and red hair). This data will establish whether the level of melanin plays a role in methylation as well as oxidative damage in form of 8-oxo-dG. Moreover, this study will gather data concerning the genetic changes (in form of CPDs) in melanocytes and fibroblasts associated with UV exposure that arise immediate after exposure due to direct absorption of radiation.

2 Materials and Methods

2.1 Materials

2.1.1 Reagents

- Citric acid monohydrate (Sigma-Aldrich, USA)
- Crystal violet (Sigma-Aldrich, USA)
- dbCAMP (Sigma-Aldrich, USA)
- EDTA (American Bioanalytican, USA)
- Fetal Bovine Serum (FBS) (Hyclone, ThermoScientific, USA)
- H_2O_2 (T.J Baker, USA)
- H_2O (DNA and RNA free) (American Bioanalytican, USA)
- H_2SO_4 (T.J Baker, USA)
- Heparin-Sodium Salt (Sigma-Aldrich, USA)
- HCl (Sigma-Aldrich, USA)
- Human Fibroblast Growth Factor (VWR, USA)
- Horse serum (GemCell, USA)
- 3-isobutyl-1-methylxanthine (IBMX) (Sigma-Aldrich, USA)
- Methanol (T.J Baker, USA)
- Na_2HPO_4 (Sigma-Aldrich, USA)
- Na_3VO_4 (Sigma-Aldrich, USA)
- NaOH (Sigma-Aldrich, USA)
- o-phenylene diamine (Sigma-Aldrich, USA)
- o-Phenylenediamine dihydrochloride (Sigma-Aldrich, USA)
- Phosphate Buffered Saline 1X (Dulbeco, Sigma Aldrich, USA)
- Penicillin Streptomycin (Gibco, USA)
- Propidium iodide (Sigma-Aldrich, USA)
- Protamine sulphate (Sigma-Aldrich, USA)
- 12-O-tetradecanoylphorbol-13-acetate (TPA) (Sigma-Aldrich, USA)

- Tris-HCl (American Bioanalytican, USA)
- Trypan blue (ThermoScientific, USA)
- Tween-20 (Sigma-Aldrich, USA)

2.1.2 Equipment

- CellCountess Cell counter (ThermoScientific, USA)
- Centrifuge GS-6R (Beckman, USA)
- Cetrifuge 5417C (Eppendorf, USA)
- Comet gel apparatus (Trevigen, USA)
- Incubator (VWR, USA)
- Incubator C02 Water Jacketed (FormaScientific, USA)
- NanoDrop WD-1000 spectrophotometer (ThermoScientific, USA)
- Power supply for gel apparatus (VWR, USA)
- PTC-100 Programmable Thermal Cycler (BioRad, USA)
- Standard Heatblock (VWR, USA)
- Virsonic 60 sonicator (Virtis,USA)

2.1.3 Other Equipment

- 10 cm dish (BD Falcon, USA)
- 15, 50 mL tubes (BD Falcon, USA)
- 2 mL tubes (Eppendorf, USA)
- 2-well Cell culture slides (BD Falcon, USA)
- 6-well plates (BD Falcon, USA)
- 96 Well Optical Bottom black Wall Plates (Nunc, ThermoScientific USA)
- 96 Well polyvinylchloride flat-bottom microtiter plates (Fisher, USA)
- Cell counting slides (Thermoscientific, USA)
- Cell scraper (BD Falcon,USA)

2.2 Methods

2.2.1 Cell culture

2.2.1.1 Human melanocytes

Normal human epidermal melanocytes from neonatal Caucasian foreskin were supplied by Dr. Ruth Halaban, Dept. Dermatology, Yale School of Medicine. Cells were split when they reached ~80% confluency. Cells were fed 2 times per week with Human melanocyte medium (OptiMem base+glutamine containing 5% FBS, 10ng/mL hFGF, 1ng/mL Heparin, 0.1M dbCAMP, 10mM IBMX, and 1% PenStrep (10,000 U/mL Penicillin and 10,000 µg/mL Streptomycin)).

2.2.1.2 Mouse melanocytes

2.2.1.2.1 C57BL/6 black melanocytes

For initial experiments, immortalized C57BL/6 melanocytes were used because of their easy handling and rapid cell divisions. Cells were provided by Dr. Ruth Halaban. Culture conditions were as described above except the medium was OptiMem base+Glutamine containing 7% Horse Serum, 16.5nM TPA and 1% PenStrep. Cells were fed 2 times per week.

2.2.1.2.2 C57BL/6 MC1R (e/e) melanocytes

Normal murine epidermal melanocytes from neonatal C57BL/6 MC1R (e/e) mice were supplied by Dr. Marcus Bosenberg, Dept. Dermatology, Yale School of Medicine. Cells were grown in OptiMem base+glutamine containing 200 nM TPA, 1% PenStrep, 5 % FBS, 1 X Non Essential Amino acids and 200 nM Cholera toxin.

2.2.1.2.3 129S1 albino melanocytes

Normal murine epidermal melanocytes from neonatal albino 129S mice were supplied by Dr. Marcus Bosenberg, Dept. Dermatology, Yale School of Medicine. Cells were grown in OptiMem base+glutamine containing 16nM TPA, 1% PenStrep, 5 % FBS, 7% Horse Serum.

2.2.1.3 Human Fibroblasts

Human fibroblasts were obtained from neonatal foreskin and provided by Dr. Ruth Halaban. Cells were cultured in media with DMEM F12 base containing 10%FBS and 1% PenStrep.

2.2.2 UV exposure

Melanocytes were seeded in 10 cm dishes at a density of 1,000,000 cells/dish. Forty-eight hours later, medium was removed and plates were washed with PBS. Cells were covered with 4 mL PBS and immediately exposed to UV. Each experiment included un-exposed control cells. Immediately after exposure, PBS was removed and cells were either immediately scraped using a cell scaper (BD Falcon, USA) and counted for a 0 hour time point or kept in the culture medium for 24 h, 48 h, 72 h, (7days) for further experiments.

2.2.2.1 nbUVB

Two TL20W/01 PHILIPS UVB Narrowband UVB lamps (Solarc Systems, CANADA) which have a peak at 311 nm and nearly 0 output outside 305-315 nm were used as a source. Total emitted fraction measured with a UV Products, Inc. UVX meter was 17% UVA, 81% UVB and 2% UVC with an nbUVB output of 2.9 W/m^2. Some or all of the UVA and UVC readings may result from the UVA and UVC probes' known cross-sensitivity to UVB rather than actual presence of these wavelengths in the output. The spectrum provided by Philips indicates 0 output in the UVA and UVC. Accordingly the exposure times were 2 min 52 s (for 500 J/m^2) to 70 min (for 12,000 J/m^2).

2.2.2.2 UVA

The UVA source consisted of eight TL20W/01 UVA bulbs (Solarc Systems, CANADA)) with an output of 65 mW/cm^2. The bulb output was filtered through an 11 mm glass plate filter to remove UVB and UVC. Accordingly the exposure times were 6 min 24 s for 25 kJ/m^2 and 25 min 30 s for 100 kJ/m^2, respectively. To minimize overheating and artificial damage of the cells, all the exposures were done on ice.

2.2.3 Cell survival

2.2.3.1 Colony assay

Immediately after UV exposures, cells were trypsinized with 0.25% trypsin-EDTA and washed with PBS. Cells were stained with Trypan blue and counted on an automatic cell counter (CellCountess, ThermoScientific, USA) and plated in a 6-well culture plate at 500, 250 and 125 cells per well in duplicate. After 6 days the colonies were washed twice with ice cold PBS and fixed using ice cold methanol for 10 minutes. The colonies were stained with 0.5% crystal violet in methanol for 10 minutes. Excess stain was poured off and colonies rinsed twice with ddH_2O. Plates were allowed to dry overnight and colonies were counted the following day.

Due to their limited cell divisons/survival and inability to grow at low density, cell survival in primary cells (human melanocytes and fibroblasts) was assessed using CellTiter-Glo® reagent (Promega, USA). CellTiter-Glo® detects the presence of ATP, which corresponds to metabolically active and healthy cells. UV exposed and non-exposed cells were trypsinized and seeded at a density of 500 and 5000 cells/well into 96-well clear bottom black wall plates. Cells were allowed to grow undisturbed for 6 days post exposure. A volume of CellTiter-Glo® equal to that of the culture media was added into each well of the 96-well culture plate followed by 5 minutes incubation at room temperature. Reaction between CellTiter-Glo® substrate and ATP molecules was recorded in the form of luminiscence using a VICTOR™ luminescence plate reader (PerkinElmer, USA).

2.2.3.2 Flow cytometry

Flow Cytometry was performed to calculate the percentage of dead cells at different time points post UV exposure. Cells were exposed to nbUVB (0-12000 J/m2) and harvested 0 and 48 hr post exposure. Cells were washed in PBS and stained with 1 µmg/mL Propidium iodide (Invitrogen, USA). The stained cells were analyzed by Flow cytometry using a FACSCalibur instrument (BD Biosciences, San Jose, CA) equipped with CellQuest 3.3 software and later analyzed using FlowJo (Tree Star, USA).

2.2.4 DNA damage

2.2.4.1 Comet assay

The Comet assay was performed using the CometAssay kit (Trevigen Inc, USA). Briefly, exposed and non-exposed control cells were collected and resuspended in PBS. Approximately 300-500 cells were combined with low melting agarose and pipetted immediately onto pre-warmed CometSlides (Trevigen, USA). After the agarose had polymerized, slides were lysed in pre-chilled lysis solution (0.26N NaOH, 1.2M NaCl, 100mM EDTA, 0.1 % Sodium Lauroyl Sarcosinate, 1% Tween 20) for 2 hrs at 4°C. Following lysis, the slides were immersed in 3 changes of 1X FLARE Buffer (Trevigen Inc, USA), 10 minutes each. FpG (for 8-oxo-dG and other oxidative lesions) and Ultraviolet Damage Endonuclease (UVDE) enzymes (for CPD) were added to the slides in a dilution of 1:10 in REC BUFFER (1 X FLARE containing BSA). Slides were covered with a cover slip and incubated in a humidified chamber at 37°C for 30-45 min. The cover slips were removed and DNA was allowed to unwind in alkaline solution (100 mM NaOH, 1 mM EDTA, pH 12.5-13) for 20 min prior to electrophoresis. Electrophoresis was conducted in alkaline solution for 30 min at 21 V and 300 mA at 4°C. After washing 3 times in ddH_2O, slides were immersed in 70% ethanol for 5 min and air dryed at 37°C for 30 minutes. DNA on the slides was then stained with SYBR Green (Trevigen, USA), diluted 1:10000 in 10mM Tris-HCl (pH 7.5) and 1mM EDTA for 30 minutes at room temperature. The comets objects were observed and photographed at 10x magnification in a fluorescence microscope (AxioVert, ZEISS,USA) attached to a

camera (AxioCam MRm, ZEISS,USA). Comets in the photographs were observed and evaluated using Autocomet (TriTek, USA). Tail moments of 50 cells were measured automatically and plotted as mean values using GraphPad Prism.

2.2.4.2 ELISA

DNA was isolated using a commercially available DNA isolation kit (QUIAGEN, USA). DNA concentration was determined spectrophotometrically using a NanoDrop instrument and diluted in PBS to 2 ng/µL. DNA was heat denatured at 95°C for 7 min and snap cooled on ice. Denatured DNA was coated onto polyvinylchloride flat-bottom microtiter plates precoated with 0.003% protamine sulphate. After complete drying at 37°C over night, plates were washed five times with PBS containing 0.05% Tween-20 (PBST) and incubated with blocking solution (5%FBS in PBS) for one hour at 37°C. The plates were washed in PBST and incubated for 1hr at 37°C with primary antibodies specific for photoproducts like CPDs (CosmoBio, Japan), or 8-Oxo-dG (Trevigen, USA), at a dilution 1:700 for both antibodies in dilution buffer (5% FBS containing 0.05% Tween-20 in PBS). Plates were washed 5 times with PBST followed by 30 minutes incubation at 37°C in anti-mouse biotin-F(ab')2 fragment (Zymed, Chile) secondary antibody. To detect the Biotin, plates were then incubated for 30 min at 37°C with 1:10000 dilution of Peroxidase conjugated streptavidin. After final washing with PBST, plates were washed once in Citrate-Phosphate buffer [Citric acid monohydrate, Na2HPO4 in ddH_2O pH 5.0]. Plates were incubated for 10 minutes with o-phenylene diamine in Citric acid buffer as a substrate for peroxidase. After the appropriate color intensity appeared, the reaction was stopped with 2M H_2SO_4. Finally, absorbance of every well at 490 nm was read using a Gene 5™ microplate reader (BioTek, USA).

In order to minimize oxidative background for the 8-oxo-dG samples, nuclei were isolated prior to DNA isolation with a hypotonic solution (10 mM HEPES pH 7.4-7.9, 10 mM KCL, 1.5 mM $MgCl_2$, 0.1% NP-40) supplemented with antioxidants (5mM Desferal, 1mM Reduced Glutathine, 3 mM L-Histidine, all from Sigma USA). DNA isolation was done with a Qiagen Kit as described above.

2.2.5 Generation of Reactive Oxygen Species (ROS)

Total ROS production after H_2O_2 treatment, nbUVB, or UVA exposure was measured using the indicator dye CM-H_2DCFDA (Invitrogen, USA). This dye is cell membrane permeable and non fluorescent until intracellular esterases cleave the acetate group. The remaining molecule reacts with intracellular ROS and starts fluorescing. C57BL/6 melanocytes were exposed to nbUVB or UVA. Total ROS and mitochondrial superoxide were detected by incubating cells with 25 µM CM-H_2DCFDA for 20 min at 37°C. The fluorescence for oxidized CM-DCFDA (Ex/Em = 495/529 nm) was measured using a fluorescence plate reader (Synergy, BioTek ™, USA). As a positive control, cells were washed and incubated in 200 µM H_2O_2 for 20 min at 37°C, then washed and treated with the dye as stated above.

2.2.6 Methylation assay (MBD pull down)

Genomic DNA was sonicated on a Virsonic 60 sonicator, twenty-five cycles at a 6W output setting. The sonication was performed on ice and each pulse was 10 seconds with a gap of 5 seconds between each pulse. The DNA was purified using a Qiaquick PCR purification kit (Qiagen, USA). The concentration of purified DNA was measured using a NanoDrop instrument and used for methylated DNA pull down by a His-tagged MBD2 protein. Binding was performed in binding buffer for 30 minutes as prescribed in the Dynabeads protocol (Invitrogen, USA). The beads bound to MBD protein (along with the captured DNA fragments) were washed 5 times with washing buffer. The unbound fraction was saved for later validation and the bound fraction was purified again using the Qiaquick kit and finally eluted. The sonicated and purified DNA was used in a quantitative PCR reaction to validate the enrichment of methylated DNA. The beta actin promoter region was used as the target amplicon for unmethylated DNA and the heavily methylated IAP region was used as the enrichment control. Relative enrichment was established by comparing the cycle threshold value (CT) in a real-time PCR reaction. The MBD pulled-down DNA was then amplified using a chromatin immunoprecipitation assay protocol (Affymetrix, USA). The amplified DNA was tested again by quantitative

PCR as described above for maintenance of enrichment and to rule out amplification bias. The amplified targets were sent to the Vermont Cancer Center microarray core facility to be fragmented, labeled, and hybridized to the Mouse Promoter 1.0 R tiling array (Affymetrix, USA).

3 Results

3.1 Cell survival

Propidium iodide (PI) was used to determine the UV induced cell death in C57BL/6 Melanocytes, because dying cells become porous membranes thus allowing PI to enter and stain the nucleus. Following PI staining Flow Cytometry was utilized to estimate an initial nbUVB dose for ~70% C57BL/6 melanocytes survival post exposure. The first experimental nbUVB doses used were 2000, 4500, 7000, 9500 and 12000 J/m^2. It was observed that a dose of 4500 J/m^2 kills approximately 40% of cells by 48 hr after exposure to nbUVB, whereas higher doses killed 100% (Fig. 5). The preliminary PI data suggested an nbUVB dose between 500 to 2000 J/m^2 for 70% survival post UV exposure.

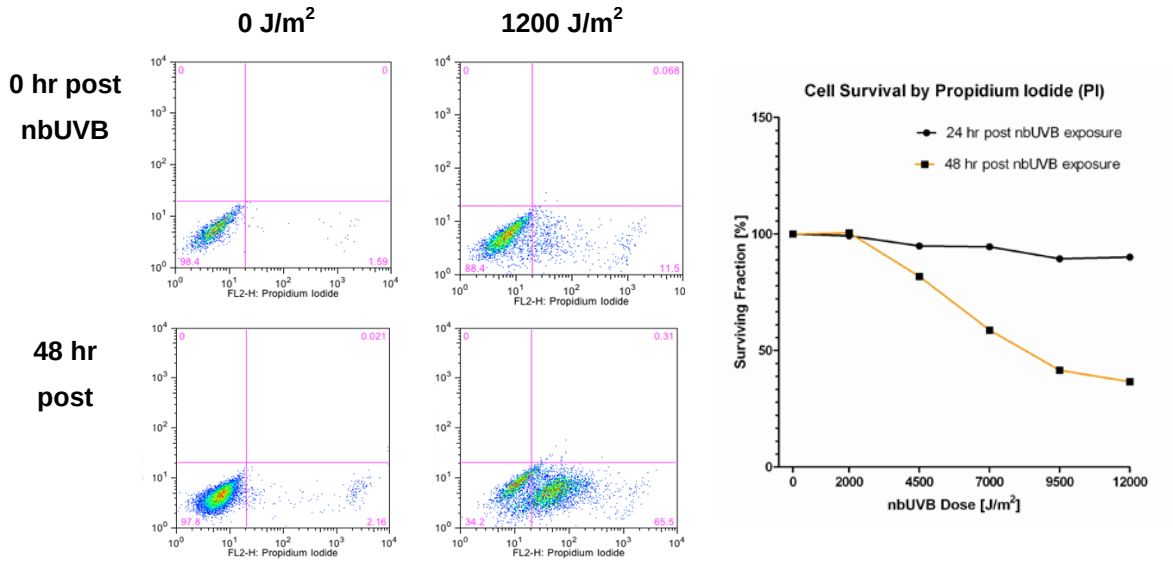

Fig. 5: a) Cell survival for C57BL/6 exposed to nbUVB. Cells were irradiated with 1200 J/m^2 nbUVB and kept for 0 hr and 48 hr post UV. Cells were collected and stained for PI. The fluorescence for PI is displayed on the x-axis**. b)** Survival fraction at 2000 J/m^2, 4500 J/m^2, 7000 J/m^2 and 9500 J/m^2.

However, UV exposure itself may cause leaky membranes, allowing PI to enter live cells and ultimately leading to false positives. Thus, a colony formation assay was adapted as an alternate. The colony forming ability of C57BL/6 melanocytes in response to nbUVB and UVA exposure suggested 70% cell survival doses which were approximately 1250 J/m^2 and 50-75 kJ/m^2 for nbUVB and UVA, respectively (Fig. 6). For UVA exposure, doses were adapted from the literature on human fibroblasts and keratinocytes and tested on C57BL/6 melanocytes, to see whether melanin and murine origin alter the suggested dose. The dose range for UVA was 25 to 200 kJ/m^2. These doses were independently reconfirmed with CellTiter-Glo®, a luminiscence metabolic assay that measures the ATP content of living cells (Fig. 6). Survival curves for human fibroblasts (Fig. 7) indicated the same doses as mentioned above. Ionizing radiation such as UV exhibits a cell survival curve that is almost a straight line in a logarithmic plot. However, the present survival curves exhibit a broad shoulder indicating that the used cells are to some extent resistant to UV.

a)

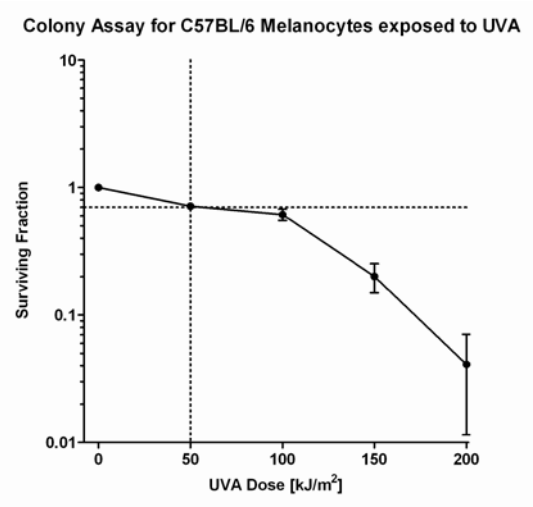

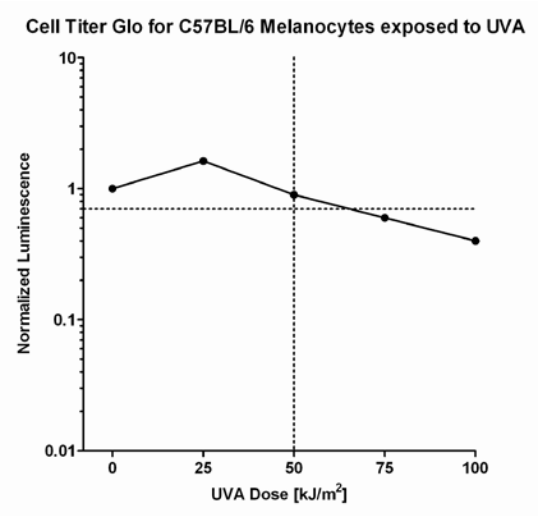

b)

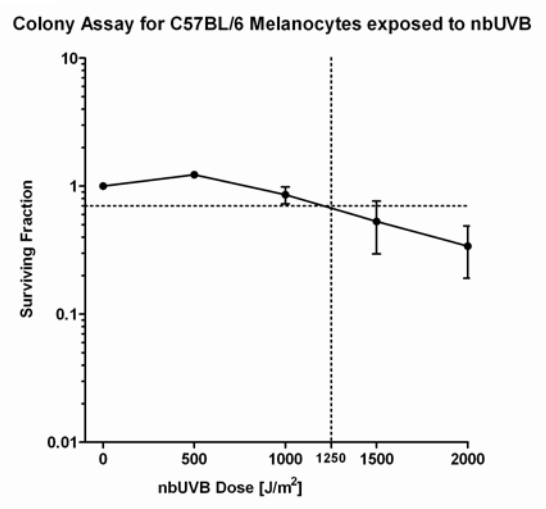

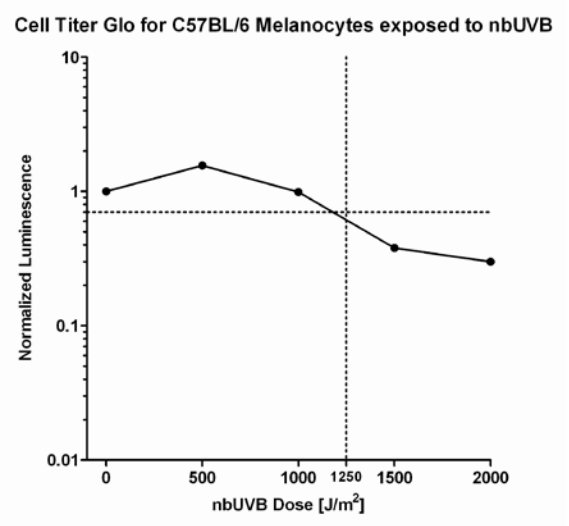

Fig. 6: Survival curves for immortalized C57Bl/6 melanocytes irradiated with **a)** UVA and, **b)** nbUVB measured 6 days after exposure using colony assay and CellTiter-Glo®.

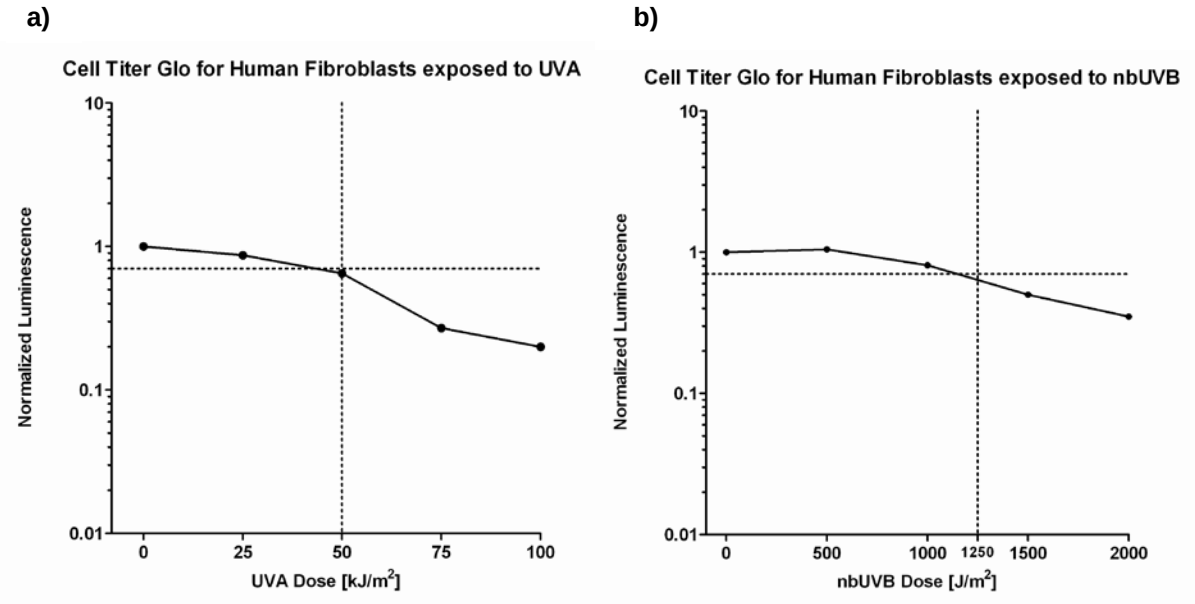

Fig. 7: Survival curves for Human fibroblasts irradiated with **a)** UVA and, **b)** nbUVB measured 6 days after exposure using CellTiter-Glo®.

3.2 DNA damage

3.2.1 ELISA

3.2.1.1 CPD

Three cell types, namely C57BL/6 melanocytes, human fibroblasts and human melanocytes, were exposed to both nbUVB and UVA. As a well-studied lesion, CPDs were studied first as a control for future studies of oxidative lesions. The rate of CPD induction in C57BL/6 melanocytes (Fig. 8). (Tables 1, 2) and human fibroblasts (Fig. 9) (Tables 3, 4) is apparently linear with dose in the tested regions for both UVA and nbUVB 0 hr post UV. The unexposed (0 J/m^2) samples showed a low CPD background in contrast to CPDs in exposed samples.

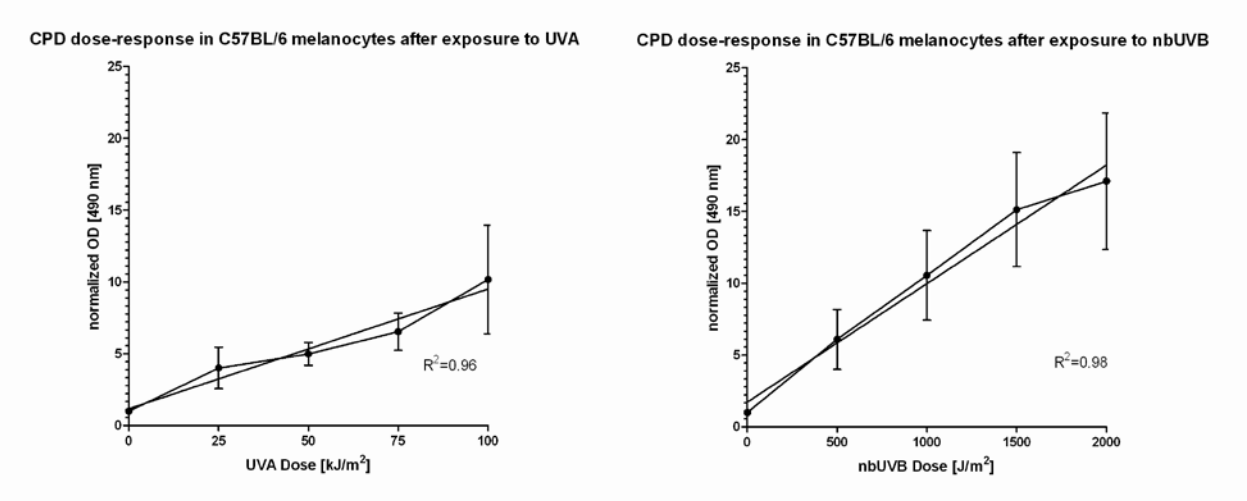

Fig. 8: Formation of CPDs in C57BL/6 melanocytes exposed to UVA and nbUVB at 0hr post UV exposure. The y axis value is the OD reading produced by an ELISA assay. Data points are mean values of at least 4 independent experiments, including standard error of the mean (SEM). The correlation coefficient calculated by linear regression of mean values is 0.96 for C57BL/6 melanocytes exposed to UVA and 0.98 for C57BL/6 melanocytes exposed to nbUVB.

Table 1: UVA-induced increase in CPD in C57BL/6 Melanocytes

UVA dose [kJ/m^2]		X fold increase
0	(n=4)	1
25	(n=4)	4
50	(n=4)	5
75	(n=4)	6.5
100	(n=4)	10

Table 2: nbUVB induced increase in CPD in C57BL/6 Melanocytes

nbUVB dose [J/m^2]		X fold increase
0	(n=4)	1
500	(n=4)	6
1000	(n=4)	10.5
1500	(n=4)	15
2000	(n=4)	17

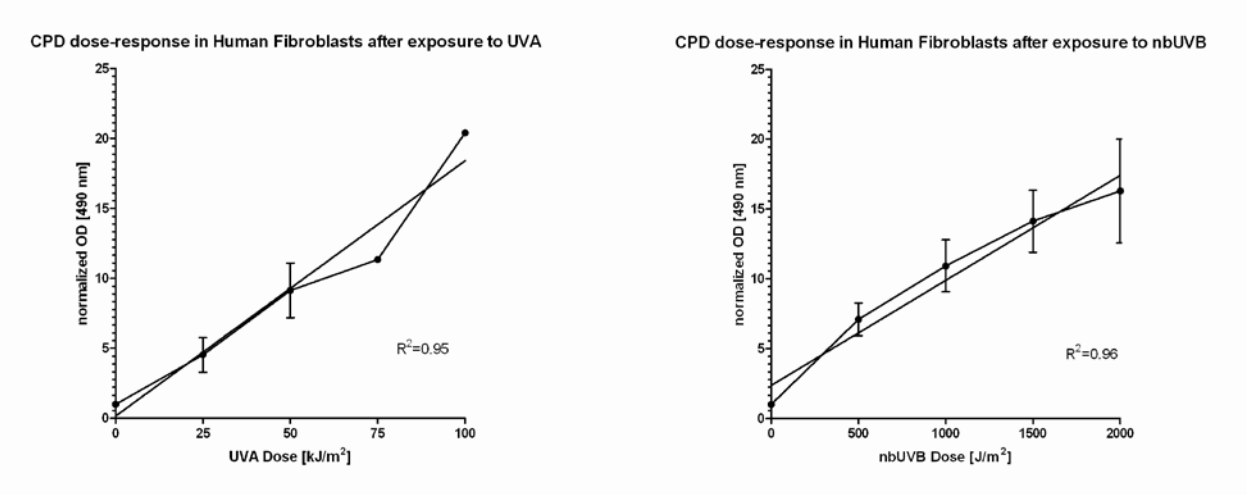

Fig. 9: Formation of CPDs in human fibroblasts 0hr post exposure to UVA or nbUVB. Mean values of at least 4 independent experiments including standard error of the mean (SEM) are given. The correlation coefficient calculated by linear regression of mean values is 0.95 for human fibroblasts exposed to UVA and 0.96 for C57BL/6 melanocytes exposed to nbUVB.

Table 3: UVA-induced increase in CPD in Human Fibroblasts

UVA dose [kJ/m^2]		X fold increase
0	(n=2)	1
25	(n=2)	4
50	(n=2)	9
75	(n=1)	11
100	(n=1	20

Table 4: nbUVB induced increase in CPD in Human Fibroblasts

nbUVB dose [J/m^2]		X fold increase
0	(n=4)	1
500	(n=4)	7
1000	(n=4)	11
1500	(n=4)	14
2000	(n=3)	16

This data suggests that the initial CPD levels in C57BL/6 melanocytes after UVA exposure were less than with nbUVB exposure. In contrast, the initial CPD levels were almost comparable to each other in human fibroblasts after nbUVB and UVA.

Next, CPD formation and repair in individual cell types was studied over the course of several time points ranging from 0h, 4h, and 12h to 7 days, using an ELISA assay. Figure 10 shows the CPD repair curves for C57BL/6 melanocytes over time from 0 hr to 168 hr post (a) UVA or (b) nbUVB exposure. For both UV exposures different doses were used, 0-100 kJ/m^2 for UVA, and 0-2000 J/m^2 for nbUVB. The non specific background while performing ELISA was subtracted and all doses at each time point were normalized to their own 0 J/m^2 control. Interestingly, dimers were highest 4 hours post UVA exposure in 4 independent experiments. In contrast, this peak at 4 hours was not observed in melanocytes exposed to nbUVB, although it may be present as a shoulder in the time course. Only ~50% of CPDs were removed after 48 hr post UVA and nbUVB exposure. Even after 7 days post exposure ~20% CPDs remained unrepaired. . Different doses for human melanocytes could not be examined due to the limited number of cells available as a result of their limited cell growth.

In contrast, the human fibroblasts and human melanocytes removed approximately 50% of CPDs in the first 12 hr post exposure to UVA or nbUVB (Fig. 12). CPDs were repaired at a significantly faster rate in human melanocytes compared to human fibroblasts. Human fibroblasts showed 80% of CPDs remaining after 12 hrs, whereas only 40-50% remained in human melanocytes for both UV types in the same amount of time.

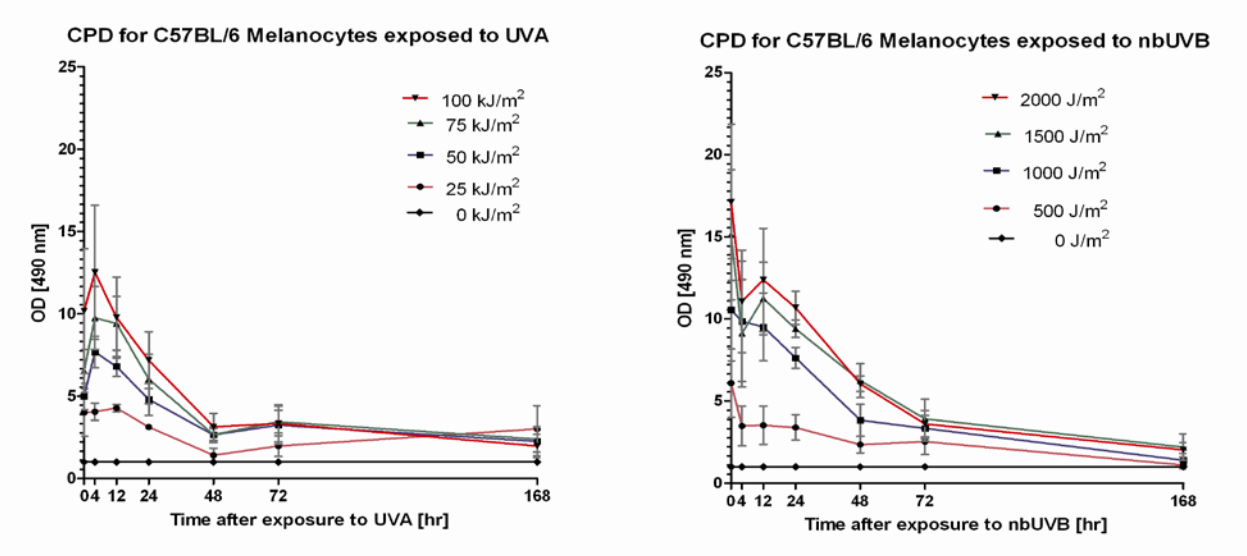

Fig. 10: Time course of induction and repair of CPD photoproducts. C57BL/5 melanocytes were exposed to **a)** UVA (0-100 kJ/m^2) or **b)** nbUVB (0-2000 J/m^2) and allowed to repair for different time periods, 4,12,24,48,72 and 168 hr. OD units are corrected for cell dilution due to cell duplication. Each color is representing a different does and each dose was repeated in four independent experiments. Values are displayed as mean (normalized to 0 J/m^2 for each time point) ± standard error of the mean (SEM). The mean ODs for unirradiated cells (0 J/m^2) are presented as a black line at the bottom.

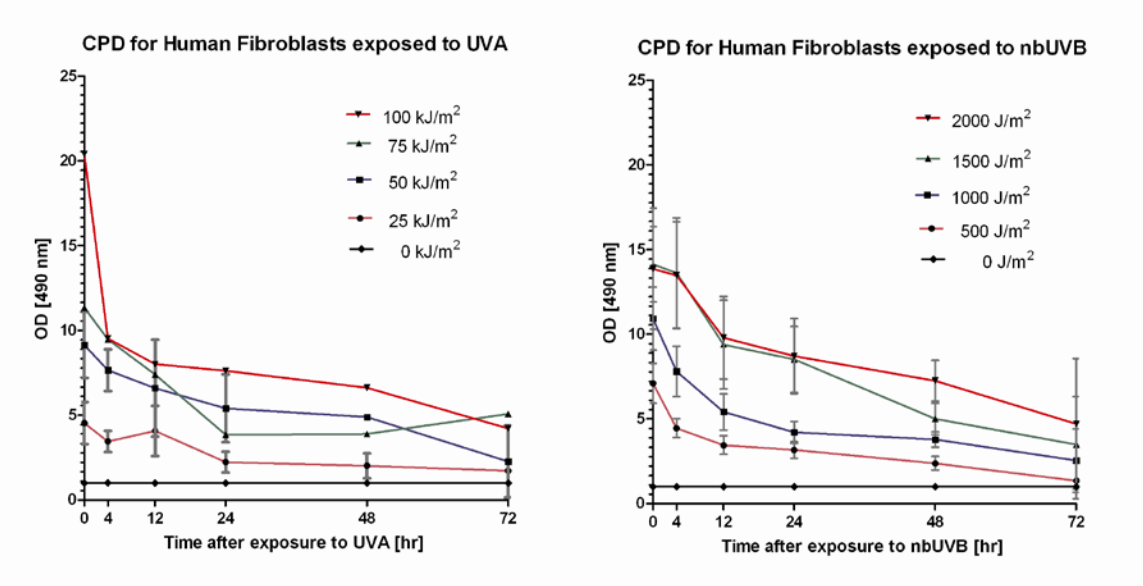

Fig. 11: Repair of CPD photoproducts. Human fibroblasts were exposed to **a)** UVA (0-100 kJ/m^2) or **b)** nbUVB (0-2000 J/m^2) and allowed to repair for different time periods, 4,12,24,48 and 72 hr. Two independent experiments were performed and values are displayed as mean (normalized to 0 J/m^2 for each time point) ± standard error of the mean (SEM). The mean ODs for unirradiated cells (0 J/m^2) are presented as a black line at the bottom.

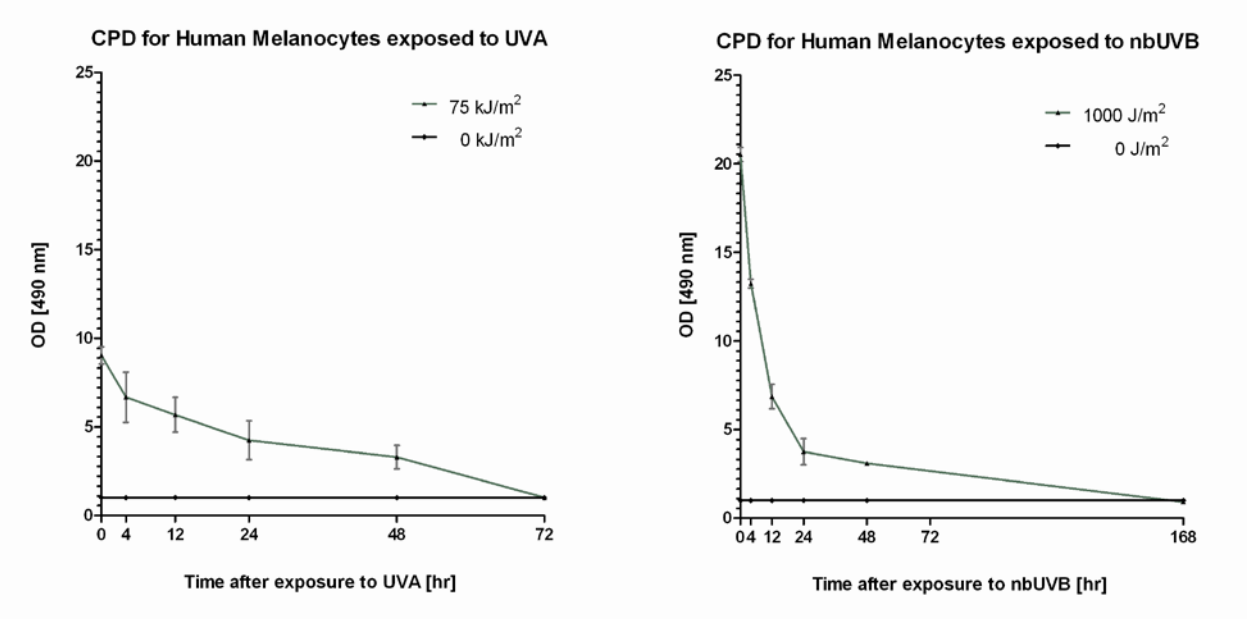

Fig. 12: Repair of CPD photoproducts. Human melanocytes were exposed to **a)** UVA (75 kJ/m^2) or **b)** nbUVB (1000 kJ/m^2) and allowed to repair for different time periods, 4,12,24,48 and 72 hr. Two independent experiments were performed and values are displayed as mean (normalized to 0 J/m^2 for each time point) ± standard error of the mean (SEM).

3.2.1.2 8-oxo-dG

Induction and repair of the 8-oxo-dG oxidative lesions following UVA and nbUVB in C57BL/6 melanocytes is shown in Figure 13. These lesions are much less frequent than CPDs and the artificial background during their determination with ELISA was too high for any conclusive statements. Therefore a COMET-Assay for 8-oxo-dG was established, where the artificial background incurred usually during DNA isolation could be avoided.

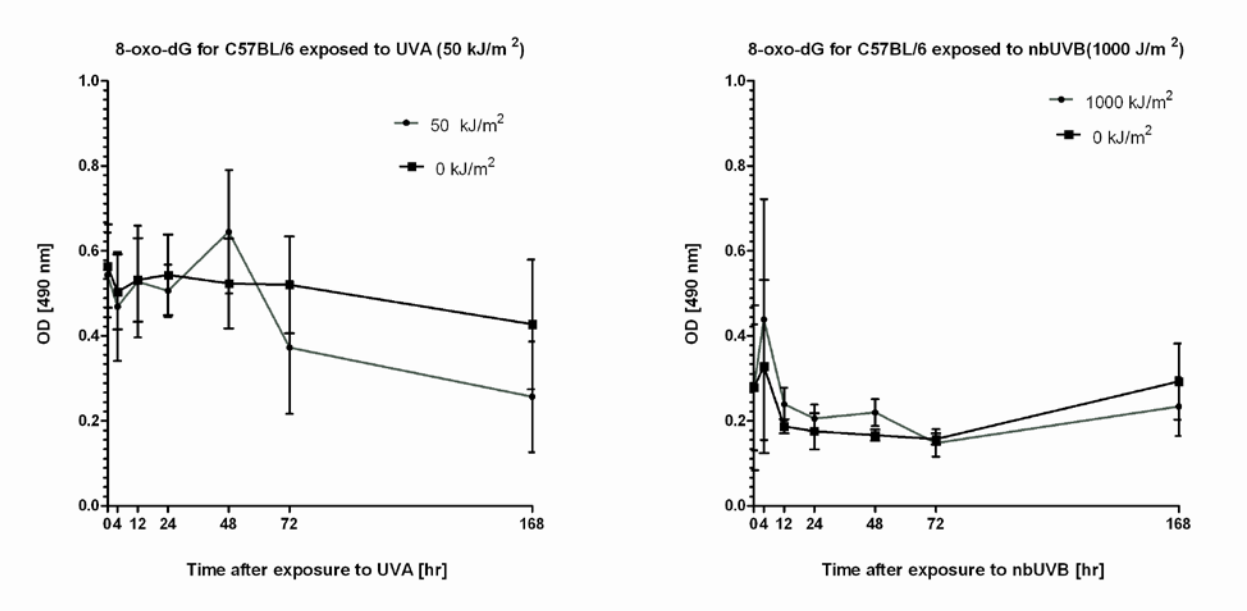

Fig. 13: Repair of 8-oxo-dG. C57BL/6 Melanocytes were exposed to **a)** UVA (75 kJ/m^2) or **b)** nbUVB (1000 kJ/m^2) and allowed to repair for different time periods, 4,12,24,48, 72 and 168 hr. Three independent experiments were performed and values are displayed as mean (normalized to 0 J/m^2 for each time point and 0 hr) ± standard error of the mean (SEM).

3.2.2 Comet assay

3.2.2.1 UVDE for CPD

The Comet assay was used to determine 8-oxo-dG and confirm the previous CPD results after nbUVB and UVA exposures to C57BL/6 melanocytes. In unexposed melanocytes the cell nucleus was dense and only a few cells showed comet tails. After exposure, a higher percentage of damaged cells, indicated by comets, could be observed (Fig. 14). These experiments display a dose response for nbUVB (Fig. 15). As expected, both the number of damaged cells exhibiting a comet and the tail moment increased in a dose dependent manner.

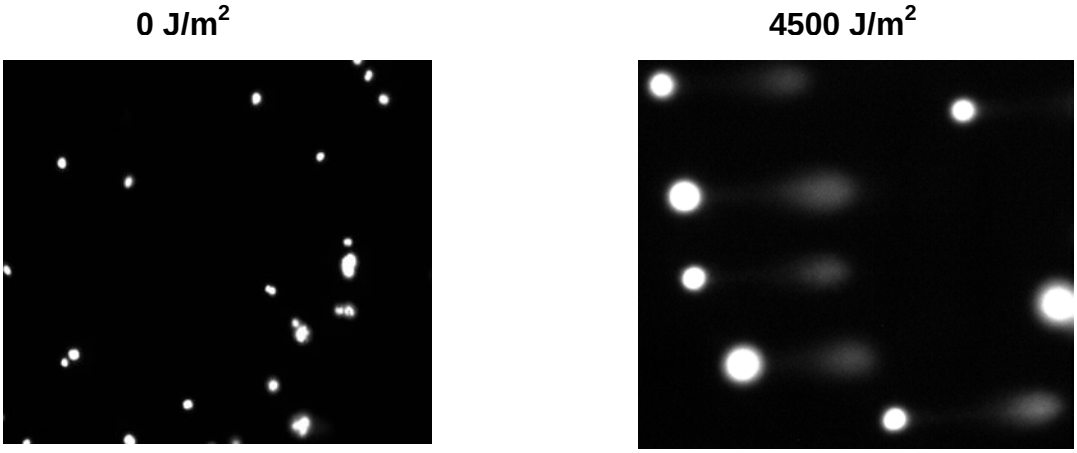

Fig. 14: UV induced CPD sites detected by Comet assay. C57BL/6 melanocytes were treated with nbUVB **a)** 0 J/m^2 (20 X) and **b)** 4500 J/m^2 (40 X) and analyzed for their tail moment. Images were taken with a fluorescence microscope (AxioVert, Zeiss, USA).

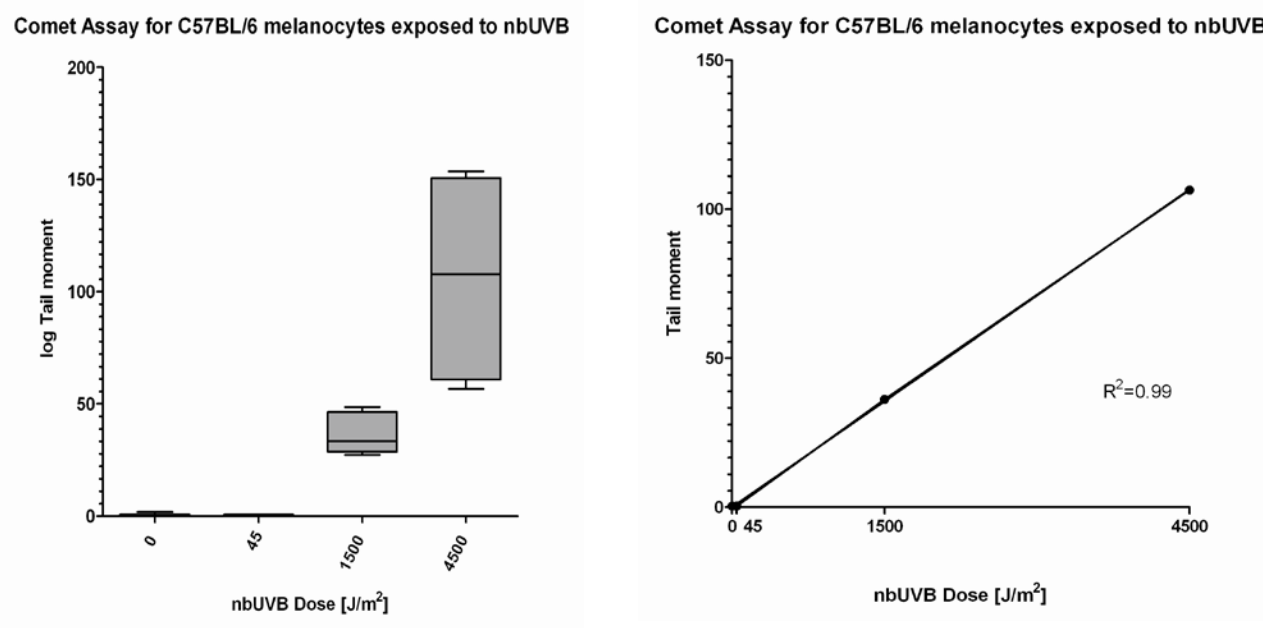

Fig. 15: Quantification of UV induced CPDs in C57BL/6 melanocytes exposed to nBUVB (0-4500 J/m^2). Comet assay. 50 nuclei were scored and their tail moment was determined.

3.2.2.2 Fpg for 8-oxo-dG

The level of 8-oxo-dG was measured by COMET-Assay for C57BL/6 melanocytes exposed to UVA (Fig. 16). The bacterial enzyme Fpg was used to study specific oxidative lesions, inlcuding 8-oxo-dG. Unexposed cells exhibited a very small tail moment (0.5±SEM 0.2), whereas cells exposed to 150 kJ/m^2 UVA had a tail moment of 20 ±SEM 1.5. Moreover, the tail moment increased in a linear manner with increasing UVA dose (Fig. 17). The overall artificial background level of oxidation was smaller than in ELISA experiments. The formation of 8-oxo-dG was also observed over a time course from 0 to 48 hr. Interestingly, the melanocytes showed a peak in 8-oxo-dG formation 4 hr post UVA exposure. Although the mouse melanocytes started to repair the 8-oxo-dG lesions between 4 and 12 hr post UVA exposure (Fig. 18), some lesions still remained even 48 hrs post UVA exposure.

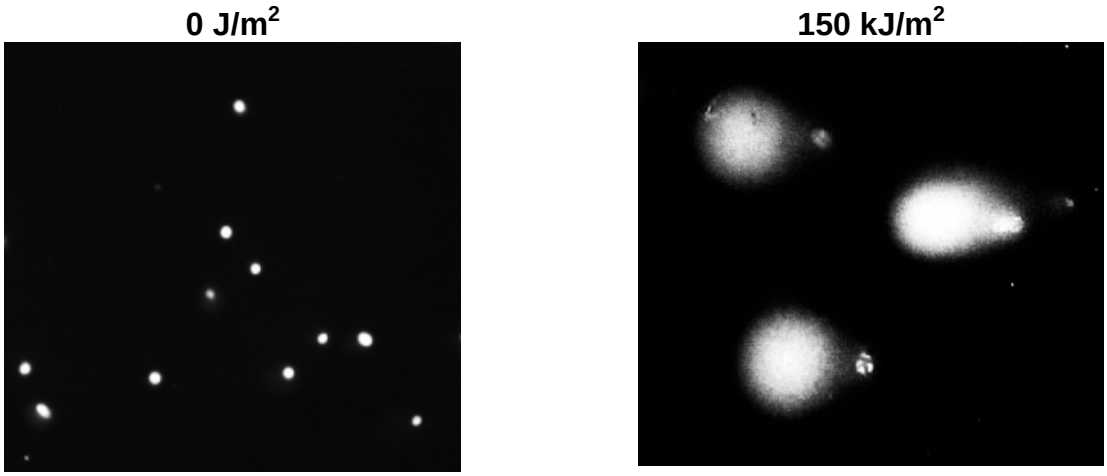

Fig. 16: UV induced CPD sites detected by Comet assay. C57BL/6 melanocytes were treated with nbUVB **a)** 0 J/m^2 (20 X) and **b)** 4500 J/m^2 (40 X) and analyzed for their tail moment. Images were taken with a fluorescence microscope (AxioVert, ZEISS, USA).

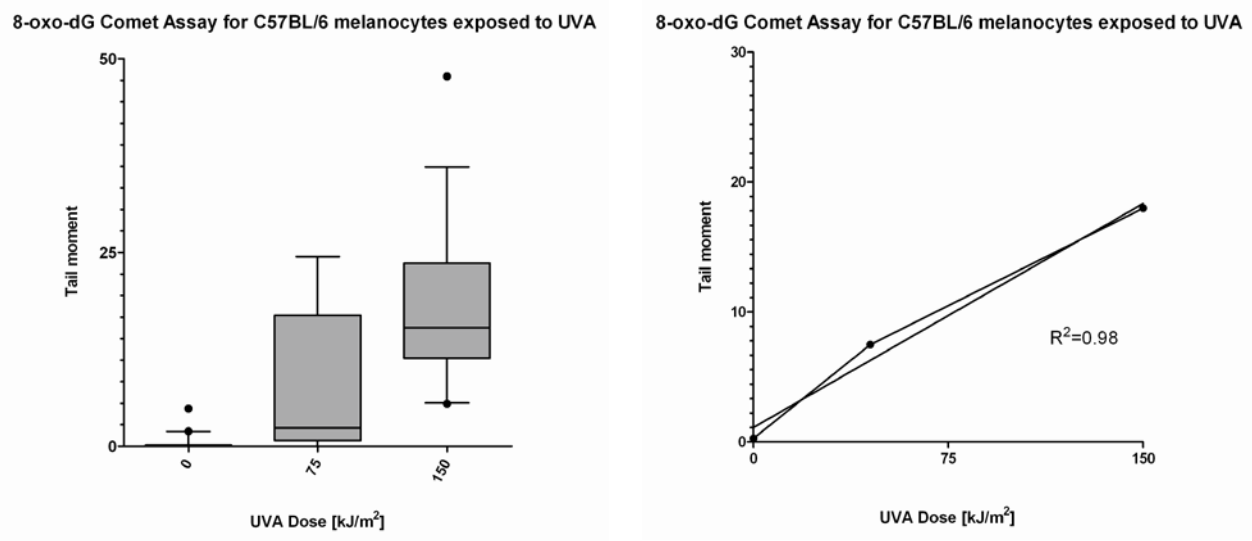

Fig. 17: Quantification of UV induced oxidative lesions in C57BL/6 melanocytes exposed to UVA (0, 75 and 100 kJ/m^2). 50 nuclei were scored and their tail moment was determined.

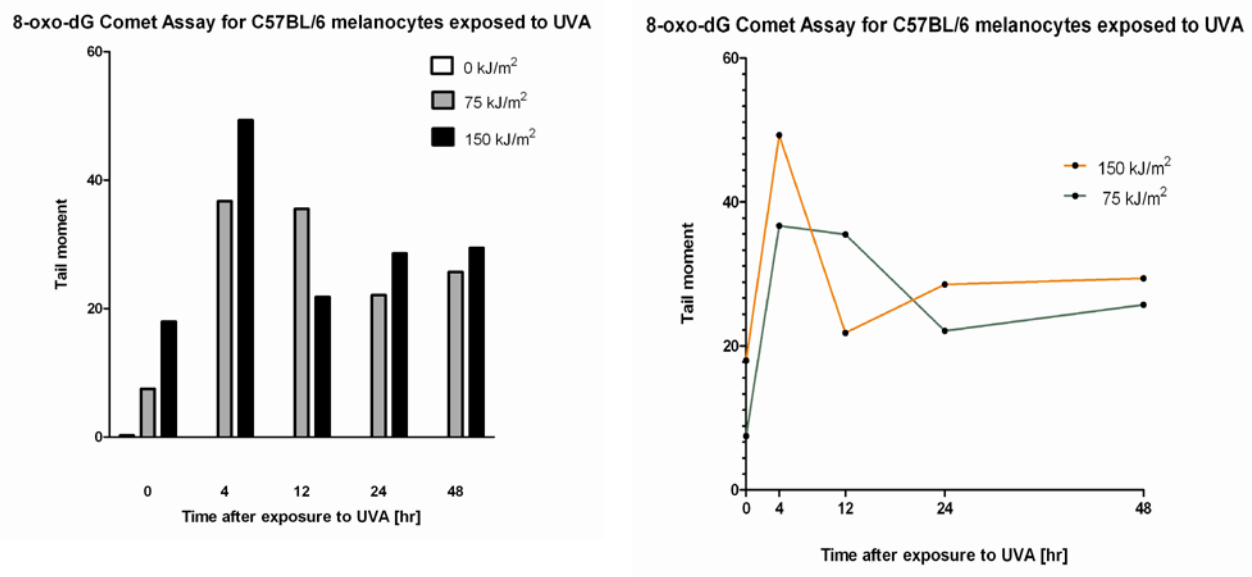

Fig. 18: Quantification of UV induced oxidative lesions in C57BL/6 melanocytes exposed to UVA (0, 75 and 100 kJ/m^2). 50 nuclei were scored and their tail moment was determined.

3.3 ROS Fluorimetry

Treatment of cells with UV resulted in elevated levels of total ROS that were detected using the fluorescent dye CM-H_2DCFDA (Fig. 19). The approximate increase in ROS levels was 2-3 fold immediately after UVA and 1.2-1.5 fold after nbUVB. The highest level of ROS was observed with 150 kJ/m^2 UVA and 1000 J/m^2 nbUVB whereas the positive control (200 µM H_2O_2) led to 4 fold increase in ROS level. The amount of ROS 3 hr post exposure to 75 kJ/m^2 is shown in Figure 20.

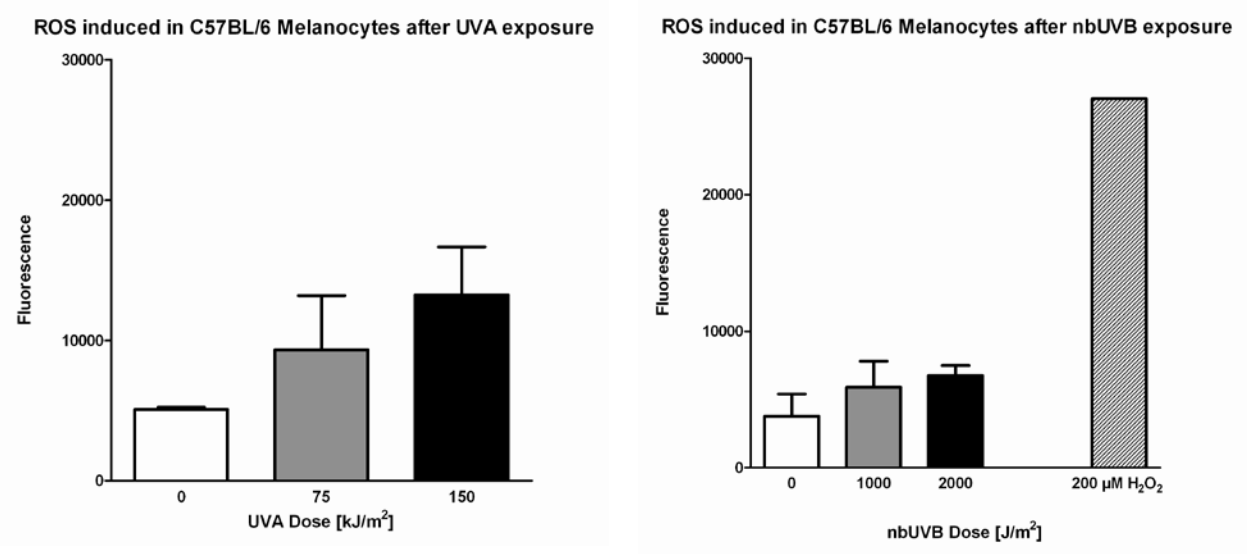

Fig. 19: Induction of total ROS by a) UVA (0-150 kJ/m2) and b) nbUVB(0-2000 J/m^2) in C57BL/6 melanocytes. Untreated cells are indicated with a white column; grey and black represent UV doses; and the dashed column represents 200 µM H_2O_2. Values are displayed as mean of two independent experiments ± SEM. The experiment using H_2O_2 as a positive control was performed once.

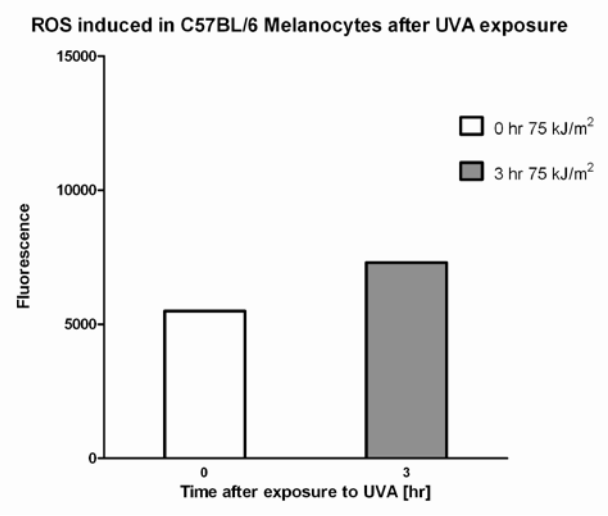

Fig. 20: Induction of total ROS by 75 kJ/m^2 UVA in C57BL/6 melanocytes. Cells 0hr post exposure are indicated with a white colum; grey represents 3 hr post UVA. Values are from a single experiment.

3.4 MBD Pull-down for methylated DNA

A preliminary assessment was done for possibly altered methylation patterns in C57BL/6 melanocyte gene promoters after nbUVB exposure. The methyl binding domain protein (MBD) was used to pull down DNA extracted from C57BL/6 melanocytes non exposed (0 J/m^2) and exposed to 1000 J/m^2 and 2000 J/m^2. DNA was validated for enrichment after pull-down using real-time PCR on two genes, Actin and IAP. All three samples showed ~2 x 10^6 fold enrichment in methylated DNA in comparison to unbound DNA (Fig. 21). Analysis of the pulled down DNA on a mouse promoter tiling array did not reveal any significant methylation specific difference between nbUVB exposed and un-exposed samples

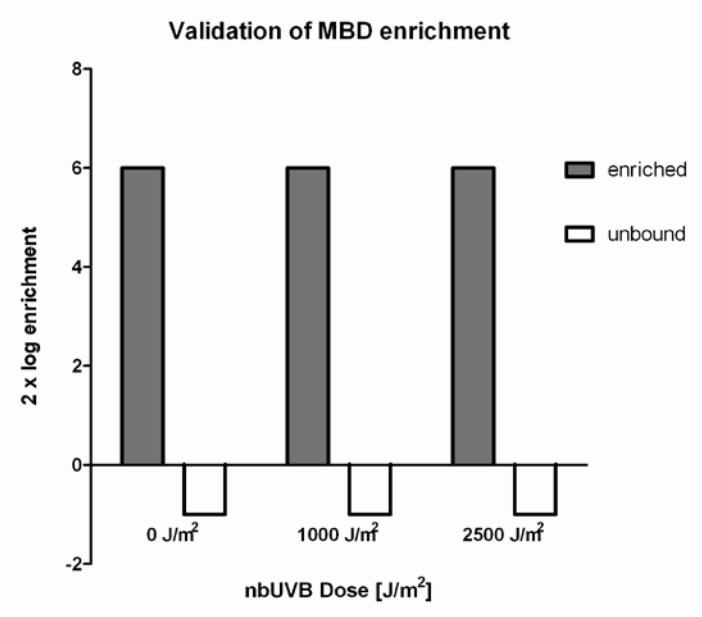

Fig. 21: Enrichment of methylated DNA after MBD binding. Grey bars indicate pulled down DNA, whereas white bars indicate DNA that was not bound to MBD protein.

4 Discussion

The path of malignant transformation in melanocytes is suggested to be a unique process because of their melanin synthesis. Melanin acts as a double edged sword since it has photoprotector/antioxidant properties while simultaneously generating ROS during melanin synthesis (MUNOZ-MUNOZ et al., 2009). In addition, melanin undergoes photolysis following exposure to UV and results in the formation of ROS (KVAM and TYRELL, 1999).

In the present study the survival of C57BL/6 melananocytes as well as human melanocytes after exposure to both UVA and nbUVB showed substantial protection mechanisms against UV indicated by the broad shoulder in the survival curves. At this point, C57BL/6 (e/e) melanocytes containing pheomelanin and 129S1 albino melanocytes are being cultured to compare the effect of pigment type on survival.

As expected, all the cell types used in this study showed immediate CPD formation post UV exposure, with a linear dose response. But interestingly, CPD formation goes further up 4 hrs post UVA exposure. The delayed CPD production may indicate a possible photosensitization phenomenon whereby the thermal decomposition of dioxetanes generates acetaldehyde and acetone (LAMOLA et al. 1971). These highly reactive molecules can then generate CPDs in the dark by triplet energy transfer, even without UV exposure. This hypothesis requires the measurements of dioxetanes and also their products acetaldehyde and acetone which are going to be measured using mass spectrometry. Human melanocytes start repairing the CPDs in first 12 hours whereas C57BL/6 melanocytes retain ~20% of the CPDs even after 7 days post UV exposure. Also, the repair in human melanocytes is faster than human fibroblasts. Fibroblasts have a seemingly low repair rate which is similar post UVA and nbUVB exposure which is consistent with D'ERRICO et al. (2003) where 70-80% CPD lesions in human fibroblasts remain 24 hr post UVB exposure.

8-oxo-dG lesions are much less frequent than CPDs. Their measurement requires a high amount of caution because of high levels of artificial background incorporated during DNA isolation, especially cell lysis. Owing to this, the COMET Assay was introduced as an alternative. The bacterial enzyme, Fpg, is specific for oxidative lesions and allows detection

of 8-oxo-dG, formamidopyrimidine (Fapy) 8-OG, 8-oxo-HG, 8-hydroxy 2 deoxyguanosine, 8-hydroxyguanine, 8-hydroxyguanosine lesions post UV exposure. This assay exhibits a low background level of 8-oxo-dG since no DNA isolation is required. As observed with CPDs, a delayed production of 8-oxo-dG can also result due to photosensitization of melanin after UV exposure. However, this experiment was performed only once and further repeats are needed for confirmation.

Total ROS levels in C57BL/6 were elevated 2 to 3 fold post UVA exposure whereas the increase was less striking with nbUVB. Also an increase in the production of ROS 4hr post UVA could be observed. This may explain the increase 8-oxo-dG 4 hr post UVA exposure. CLOTTER et al. (2007) also observed increased levels of ROS generation 4hr post UV exposure in C57BL/6 melanocytes after nbUVB exposure.

The preliminary analysis of DNA methylation by MBD pull down delivered no reliable results. A possible explanation could be that the whole genome amplification introduces a bias into the samples or the MBD protein itself did not pull down the methylated DNA reliably. Therefore, another more powerful and direct method will be adopted which is Reduced Representation Bisulfate Sequencing. The main advantages of this method are i) absence of bias since no protein or antibody is being used and ii) higher resolution at the nucleotide level.

To study the effects of different melanin levels, human melanocytes with different pigmentation backgrounds (lightly pigmented, medium pigmented and darkly pigmented) were obtained commercially. These cells will be used to determine the influence of UV on CPD and 8-oxo-dG formation according to the melanin content. Further, growth conditions were optimized for 129S albino melanocytes and C57BL/6 (e/e) melanocytes to determine the influence of pheomelanin vs eumelanin, and compare this data with C57BL/6 melanocytes.

In conclusion, the delayed photoproduct formation in C57BL/6 melanocytes after UVA exposure was surprising and thus detailed analysis of relation of ROS levels to dioxetane derivatives and photoproduct formation will be performed.

5 Summary

Melanoma is a potentially lethal form of skin cancer that arises from malignant melanocytes. The annual increase in melanoma cases in Caucasians has been estimated as 3-7%, which suggests a doubling in rates every 10-20 years (DIEPGEN and MAHLER, 2002). There is evidence that ultraviolet radiation (UV) is the main agent in causing non-melanoma skin cancer and also plays an important role in melanoma. UV radiation induces cyclobutane pyrimidine dimers (CPDs) which can lead to base changes, especially C to T and CC to TT (BRASH et al., 1991). Moreover UV, especially UVA, is absorbed by molecules with unsaturated rings leading to reactive oxygen species (ROS) production. Melanin acts as a photo protector, by scavenging ROS. However new evidence suggests that melanin is a double edged sword because ROS is generated during melanin synthesis; more precisely tyrosinase, the main enzyme catalyzing melanogenesis, is a source of hydrogen peroxide (MUNOZ-MUNOZ et al., 2009). Furthermore, UV-irradiated melanin can generate ROS (TAKEUCHI et al., 2004). The type of melanin, pheomelanin vs eumelanin, and the amount of melanin have to be considered, because pheomelanin seems to be more photosensitizing than eumelanin (WENCZL, 1998). Subsequently, these highly reactive ROS molecules can oxidize DNA and form 8-oxo-dG. ROS can also induce methylation in tumor suppressor genes, leading to a loss of function which can ultimately form tumors (LIM et al., 2008).

In this study, ELISA was used to determine the CPD formation in response to nbUVB and UVA exposure in C57BL/6 melanocytes, human melanocytes and fibroblasts. As expected, it was observed that these cell types generate CPDs immediately after exposure in a dose dependent manner. Interestingly, a peak in the production of CPDs in C57BL/6 melanocytes was observed 4 hours post UVA exposure. This delayed CPD induction may indicate the photosensitizing phenomenon observed in melanin containing cells (MOURET et al., 2006). Investigating the repair in these cells showed that human melanocytes and fibroblasts repaired 50% of CPDs in the first 12 hours after exposure, whereas C57BL/6 melanocytes repaired only 30% in the same amount of time. The formation of 8-oxo-dG was also determined using ELISA in all three cell types. A very high amount of background in 8-oxo-dG was observed at all time points (0 to 48 hr post exposure).

The COMET assay was used as an alternative method to determine 8-oxo-dG formation. The data provides evidence that 8-oxo-dGs are not repaired in the first 48hr post UVA exposure in C57BL/6 melanocytes. This may also result from repair combined with creation of new 8-oxo-dG by the same photosensitization phenomenon as mentioned above.

UV-generated ROS determined by a fluorescence based assay exhibited a dose-dependent increase in cultured C57BL/6 melanocytes immediately after exposure to UVA and nbUVB.

ROS dependent methylation was initially investigated using a MBD-Chip promoter microarray for nbUVB-exposed C57BL/6 melanocytes. Analyzing the data resulted in non-significant differences between UV irradiated and non irradiated cells. It was suggested that MBD introduces bias in the analysis of the samples. A more sensitive bisulfate sequencing assay was adapted as an alternate to MBD.

Finally, albino C57BL/6 melanocytes, C57BL/6 MC1R (e/e) melanocytes and human melanocytes with different melanin contents were established. These will be used in further studies to evaluate the role of melanin in controlling UV induced oxidative damage in cell types with different pigmentation genes.

6 Zusammenfassung

Das maligne Melanom ist eine potenziell tödliche Form des Hautkrebses, die aus bösartigen Melanozyten entsteht. Der jährliche Anstieg der Melanom-Fälle bei Kaukasiern wird auf 3-7% geschätzt. Diese Schätzungen lassen eine Verdoppelung der Raten alle 10-20 Jahre vermuten (DIEPGEN und MAHLER, 2002). Es gibt Hinweise darauf, dass ultraviolette Strahlung (UV) hauptverantwortlich für die Entstehung des weissen Hautkrebses ist und auch in der Entstehung des malignen Melanoms eine wichtige Rolle spielt. UV-Strahlung induziert Cyclobutan-Pyrimidin-Dimere (CPDs), die Basenverschiebung, insbesondere C zu T und CC zu TT (BRASH et al., 1991) verursachen können. Darüber hinaus kann UV-Exposition, insbesondere UVA, die Entstehung von reaktiven Sauerstoffspezies (RSS) verursachen, wenn diese von ungesättigten Ringen absorbiert wir. Melanin fungiert als Lichtschutz, indem es RSS abfängt. Allerdings geben neue Studien Hinweise darauf, dass Melanin als zweischneidiges Schwert betrachtet werden sollte, da RSS ebenfalls während der Melanin-Synthese erzeugt wird. Genauer gesagt, das Enzym Tyrosinase ist während der Melaninproduktion eine Quelle an Wasserstoffperoxid (MUNOZ-MUNOZ et al., 2009). Darüber hinaus kann UV-bestrahltes Melanin RSS erzeugen (TAKEUCHI et al., 2004). Weiters, sollten die Melaninform, Pheomelanin oder Eumelanin, und die Menge an Melanin in Betracht gezogen werden, da Pheomelanin mehr photosensibilisierenden Eigenschaften zu haben scheint als Eumelanin (WENCZL, 1998). Anschließend können diese hochreaktiven RSS-Moleküle DNA oxidieren und bilden 8-oxo-dG. RSS können in Folge auch Methylierung in Tumorsuppressor-Genen verursachen. Dies kann zu einem Funktionsverlust des Gens führen, welcher die Entstehung von Tumoren begünstigen kann (LIM et al., 2008).

In dieser Studie wurde ELISA verwendet, um die Bildung von CPD in Bezug auf nbUVB- und UVA-Exposition in C57BL/6 Melanozyten, humanen Melanozyten und humanen Fibroblasten zu bestimmen. Wie erwartet, wurde beobachtet, dass diese

Zelltypen CPDs unmittelbar nach der UV-Exposition in einer dosisabhängigen Weise erzeugen. Interessanterweise wurde ein Höhepunkt in der Produktion von CPDs in C57BL/6 Melanozyten 4 Stunden nach der UVA-Exposition beobachtet. Diese verzögerte CPD Induktion kann auf das photosensibilisierenden Phänomen in Melanin enthaltenden Zellen zurück gefuehrt werden (MOURET et al., 2006) Die Untersuchung der Reparatur in diesen Zellen zeigte, dass humane Melanozyten und Fibroblasten 50% der CPDs innerhalb der ersten 12 Stunden nach der Exposition reparieren, während C57BL/6 Melanozyten nur 30% in der gleichen Zeit entfernen. Die Bildung von 8-oxo-dG wurde mittels ELISA in allen drei Zelltypen bestimmt. Ein hohes Maß an nicht UV induzierten unspezifischen Hintergrundsignalen in der 8-oxo-dG Produktion wurde zu allen Zeitpunkten (0 bis 48 Stunden nach Exposition) beobachtet.
Der COMET-Assay wurde als Alternativmethode zur Bestimmung von 8-oxo-dG herangezogen. Die Daten liefern Hinweise darauf, dass 8-oxo-dG in C57BL/6 Melanozyten nicht innerhalb der ersten 48hr post UVA repariert wird. Dies kann mittels des gleichen Photosensibilisierungsphänomens, wie oben erwähnt, erklärt werden.
UV indizierte RSS wurden mittels eines Fluoreszenz bassierenden Assays bestimmt, welcher einen dosisabhängige Anstieg in kultivierten C57BL/6 Melanozyten unmittelbar nach der Bestrahlung mit UVA- und nbUVB zeigte.
Die RSS abhängige Methylierung in nbUVB exponierten C57BL/6 Melanozyten wurde zunächst mit Hilfe eines MBD-Chip Promoter Microarray untersucht. Die Analyse der Daten führte zu keinen signifikanten Unterschieden zwischen UV exponierten und nicht exponierten Zellen. Eine Bias, vermittelt durch das MBD-Protein, wird als Ursache vermutet. Als Alternative zu MBD wurde ein Bisulfat-Sequenzierungs Assay durchgefuehrt, da dieser eine hoehere Sensitivität verspricht.
Schließlich wurden albino C57BL/6 Melanozyten, C57BL/6 MC1R (e/e) Melanozyten und humane Melanozyten mit verschiedenen Mengen an Melanin etabliert. Diese werden in weiteren Studien verwendet, um die Rolle von Melanin in UV-induzierten oxidativen Schäden in Zelltypen mit unterschiedlichen Pigmentierungsgene zu evaluieren.

7 References

ADLER, A. (1942): Melanin pigment in the brain of the gorilla, Journal of Comparative Neurology **76**, 501-507

ADLER, V., YIN, Z., TEW, K.D., RONAI, Z. (1999): Role of redox potential and reactive oxygen species in stress signaling, Oncogene **18**, 6104 ± 6111

ANTEQUERA, F., BIRD, A. (1993): Number of CpG islands and genes in human and mouse, PNAS **90**, 11995-11999.

BALASUBRAMANIAN, B., POGOZELSKI, W.K., TULLIUS, T.D. (1998): DNA strand breaking by the hydroxyl radical is governed by the accessible surface areas of the hydrogen atoms of the DNA backbone,Proc. Natl. Acad. Sci. USA **95**, 9738–9743

BALL, N.J., YOHN, J.J., MORELLI, J.G., NORRIS, D.A., GOLITZ, L.E,, HOEFFLER, J.P. (1994): Ras mutations in human melanoma: a marker of malignant progression. J Invest Dermatol. **102**, 285-90.

BAYLIN, S. B., HERMAN, J. G., GRAFF, J. R., VERTINO, P. M., AND ISSA, J. P. (1998): Alterations in DNA methylation: a fundamental aspect of neoplasia, Adv Cancer Res **72**, 141

BOSE, B., AGARWAL, S., CHATTERIEE, S.N. (1989): UV-A induced lipid peroxidation in liposomal membrane, Radiat Environ Biophys **28**, 59-65

BRADFORD, P.T., GOLDSTEIN, A.M., TAMURA, D., KHAN, S.G., UEDA, T., BOYLE, J., OH, K., IMOTO, K., INUI, H., MORIWAKI, S., EMMERT, D., PIKE, K.M., RAZIUDDIN, A., PLONA, T., DIGIOVANNA, J., TUCKER, M.A., KRAEMER, K. H.(2011): Cancer and neurologic degeneration in xeroderma pigmentosum: long term follow-up characterises the role of DNA repair, J Med Genet **48**, 168-176

BRASH, D.E., RUDOLPH, J.A., SIMON, J.A., LIN, A., MCKENNA, G.J., BADEN, H.P., HALPERIN A.J., POTEN, J. (1991): A role for sunlight in skin cancer: UV induced p53 mutations in squamous cell carcinoma, PNAS **15**, 10124-10128

BRASH, D.E., SEETHARAM, S., KRAEMER, K.H., SEIDMAN, M.M., BREDBERG, A. (1987): Photoproduct frequency is not the mayor determinant of UV base substitution hot spot or cold spots in human cells, PNAS **84**, 3782-3786

BROWN, V., HARWOOD, C.A., CROOK, T., CRONIN,C., KELSELL, D.P., AND PROBY, C.M (2004): $p16^{INK4a}$ and $p14^{ARF}$ Tumor Suppressor Genes Are Commonly Inactivated in Cutaneous Squamous Cell Carcinoma. Journal of Investigative Dermatology **122**, 1284–1292

CHANDRASEKHAR, D., VAN HOUTEN, B. (2000): In vivo formation and repair of cyclobutane pyrimidine dimers and 6-4 photoproducts measured at the gene and nucleotide level in Escherichia coli, Mutat Res. **450**, 19-40

CHEDEKEL, M. R., SMITH, S. K., POST, P. W., POKORA, A. & VESSELL, D. L. (1978): Photodestruction of pheomelanin: role of oxygen. PNAS. **75**, 5395–5399.

CLAYTON, E., DOUPE, P.E., KLEIN, A.M., WINTON, D.G., SIMONS, B.D., JONES, P.H. (2007): A single type of progenitor cells maintains normal epidermis, Nature **446,** 185-189

CLYDESDALE,G., DANDIE, G., and MULLER, H. (2001): Ultraviolet light induced injury: Immunological and inflammatory effects, Immunology and Cell Biology **79**, 547–568

COTTER, M.A., THOMAS, J., CASSIDY, P., ROBINETTE, K., JENKINS, N., FLORELL, S. R., LEACHMAN, S., SMALOWSKI, W.E., GROSSMAN, D. (2008): N-Acetylcystein protects melanocytes against oxidative stress/damage and delays onset of ultraviolet-induced melanoma in mice, Clin. Cancer Res. **13**, 5952

CURTIN, J.A., BUSAM, K., PINKEL, D., BASTIAN, B.C. (2006): Somatic activation of KIT in distinct subtypes of melanoma. J Clin Oncol. **24,** 4340-6

CURTIN, J.A., FRIDLYAND, J., KAGESHITA, T., PATEL, H.N., BUSAM, K.J., KUTZNER, H., CHO, K.H., AIBA, S., BROECKER, E.B., LEBOIT, P.E., PINKEL, D.,

BASTIAN, B.C. (2005): Distinct sets of genetic alterations in melanoma. N Engl J Med, **353**, 2135-47

D'ERRICO, M.D., TESON, M., CALCAGNILE, A., DE SANTIS, L.P., NIKAIDO, O., BOTTA, E., ZAMBRUNO, G., STEFANINI M., DOGLIOTTI, E. (2003): Apoptosis and efficient repair of DNA damage protect human keratinocytes against UVB, Cell death and differentiation **10**, 754-756

DAHLGREN, C., KARLSSON, A. (1999): Respiratory burst in human neutrophils, J Immunol Methods. **17**; 3-14.

DAS, P.M., SINGAL, R. (2004): DNA methylation and cancer, Biology of neoplasia, Journal of Clin Onco. **22**, 4632-4642

DE COCK, J.G.R., VAN HOFFEN, A., WIJNANDS, J., MOLENAAR, G., LOHMAN, P.H.M., EEKEN, J.C.J (1992): Repair of UV-induced (6-4)photoproducts measured in individual genes in the Drosophila embryonic Kc cell line, Nucleic Acids Research **20**, 4789-4793

DIEPGEN, T.L., MAHLER, V. (2002): The epidemiology of skin cancer. Br J Dermatol **146** , 1-6

DOBROVIC, A., SIMPFENDORFER D. (1997): Methylation of the BRCA1 gene in sporadic breast cancer, Cancer Res **57**, 3347-3350

ESTELLER, M., CORN, P.G., URENA, J.M. (1998): Inactivation of glutathione S-transferase P1 gene by promoter hypermethylation in human neoplasia. Cancer Res **58,** 4515-4518

FEENEY-BURNS, L (1980): The pigments of the retinal pigment epithelium. In: Current Topics in Eye Research, Vol 2, ZADUNAISKY, J.A., DAVSON, H. (editors), New York, Academic Press, 119

FEINBERG, A.P., VOGELSTEIN, B. (1983): Hypomethylation of ras oncogenes in primary human cancers, Biochem Biophys Res Commun **111**, 47-54

FISHER, G.J., KANG, S., VARANI, J., BATA-CSORGO, Z., WAN, Y., DATTA, S., VOORHEES, J.J. (2002): Mechanisms of photoaging and chronological skin aging, Arch Dermatol **138,** 1462-1470

GARCIA, M.J., MARTINEZ, B., MARTINEZ, A., BENITEZ, J., RIVAS, C. (2002): Different incidence and pattern of p15INK4b and p16INK4a promoter region hypermethylation in Hodgkin's and CD30-Positive non-Hodgkin's lymphomas. Am J Pathol **161,** 1007-1013,

HALDER, R.M., BRIDGEMAN-SHAH, S. (1995): Skin cancer in African Americans. Cancer. **75**, 667–673.

HEARING, V.J., LEONG, S.P.L (2005): From Melanocytes to Melanoma: The Progression to Malignancy. Humana Press; 1 edition

HERMAN, J.G., MERLO, A., MAO, L., LAPIDUS, R.G., ISSA, J.P., DAVIDSON, N.E., SIDANSKY, D., BAYLIN, S.B. (1995): Inactivation of the CDKN2/p16/MTS1 gene is frequently associated with aberrant DNA methylation in all common human cancers. Cancer Res **55**, 4525-4530

HIDA, K. WAKAMATSU, E.V. SVIDERSKAYA, A.J. DONKIN, L. MONTOLIU AND M. LYNN LAMOREUX (20090: Agouti protein, mahogunin, and attractin in pheomelanogenesis and melanoblast-like alteration of melanocytes: a cAMP-independent pathway, Pigment Cell Melanoma Res, **22**. 623–634

HILL, H.Z., HILL, G.J. (2000): UVA, Pheomelanin and the Carcinogenesis of Melanoma, Pigment cell res **13**, 140–144

HILL, H.Z., LI, W., XIN, P., MITCHELL, D.L (1997): Melanin: A Two Edged Sword? Pigment Cell Res **10**, 158-161

IKEHATA, H., KUDO,H., MASUDA, T., ONO, T. (2003): UVA induces C-T transitions at methyl-CpG-associated dipyrimidine sites in mouse skin epidermis more frequently than UVB, Mutagenesis **18** ,511-519

JONES, P.A., BAYLIN, S.B. (2002): The fundamental role in epigenetic events in cancer, Nature Reviews Genetics ``, 415-428

KAIDBEY, K.H., AGIN, P.P., SAYRE, R., KLIGMAN, A.M. (1979): Photoprotection by melanin—a comparison of black and Caucasian skin, Journal of the American Academy of Dermatology **1**, 249-260

KLIGMAN, A.M, LAVKER, R.M. (1988): Cutaneous aging: the difference between intrinsic aging and photoaging: J cut Aging Cosm Dermatol **1**, 5-11

KLIGMAN, L.H., GEBRE, M. (1991): Chronic Ultraviolet B Irradiation Causes Loss of Hyaluronic Acid from Mouse Dermis Because of Down-Regulation of Hyaluronic Acid Synthases, Photochemistry and Photobiology **54**, 233–237

KOBAYASHI, N., NAKAGAWA, A., MURAMATSU, T., YAMASHINA, Y., SHIRAI, T., HASHIMOTO, M.W., ISHIGAKI, Y., OHNISHI, T., MORI, T (1998): Supranuclear melanin caps reduce ultraviolet induced DNA photoproducts in human epidermis, J Invest Dermatol. **110**, 806–810

KOGA, Y., PELIZZOLA, M., CHENG, E., KRAUTHAMMER, M., ARIYAN, S., NARAYAN, D., MOLINARO, A.M, HALABAN, R., WEISSMAN, S.M. (2009): Genome-wide screen of promoter methylation identifies novel markers in melanoma, Genom research **19**, 1462-1470

KVAM, E, TYRRELL, RM(1999): The role of melanin in the induction of oxidative DNA base damage by ultraviolet A irradiation of DNA or melanoma cells. J Invest Dermatol. 113:209–213

LAMOLA, A.A(1971): Production of pyrimidine dimers in DNA in the dark. Biochem Biophys Res Commun. **43**,893-8

LIM, S., GU, J., KIM, M., PARK, Y., PARK, C., CHO, J., PARK, Y., JUNG, G. (2008): Epigenetic Changes induced by reactive oxygen species in hepatocellular carcinoma: methylation of the E-cadherin promoter, Gastroenterology **135**, 2128-2140

LIPPKE, J.A., GORDON, L.K. BRASH, D.E. AND HASELTINE, W. A. (1981): Distribution of UV light-induced damage in a defined sequence of human DNA: detection of alkaline-sensitive lesions at pyrimidine nucleosidecytodine sequences. PNAS **78**, 3388-3392

LO, H.L., NAKAJIMA, S., MA, L., WALTER, B., YASUI, A., ETHELL, D., OWEN, L.B (2005): Differential biologic effects of CPD and 6-4 PP UV induced DNA damage on the induction of apoptosis and cell-cycle arrest, BMC Cancer **5**, 135.

LOEB, L., JAMES, E., WALTERSDORPH, A., KLEBANOFF, S.J. (1988): Mutagenesis by the autooxidation of iron with isolated DNA, Proc. Natl. Acad. Sci. USA **85**, 3918-3922

MCCORD, J.M. (1998): Iron, free radicals, and oxidative injury. Seminars in Hematology **35**, 5-12

MITCHELL, D.L., CLARKSON, J.M., CHAO, C.C., ROSENSTEIN, B.S. (1986): Repair of cyclobutane dimers and (6-4) photoproducts in ICR 2A frog cells. Photochem Photobiol. **43**, 595–597

MIYAMURA, Y., COELHO, S.G., WOLBER, R., MILLER, S.A., WAKAMATSU, K., ZMUDZKA, B.Z., ITO, S., SMUDA, S., PASSERON, T., CHOI, W., BATZER, J., YAMAGUCHI, Y., BEER, J.Z., HEARING, V.J. (2007): Regulation of human skin pigmentation and responses to ultraviolet radiation, Pigment Cell Research **20**, 2-13

MOURET, S., BAUDOUIN, C., CHARVERON, M., FAVIER, A., CADET, J., DOUKI, T. (2006): Cyclobutane pyrimidine dimers are predominant DNA lesions in whole human skin exposed to UVA radiation. Proc Natl Acad Sci U S A. **103**, 13765-70

MUNOZ-MUNOZ, J.L., GARCIA-MOLINA, F., VARON, R., TUDELA, J., GARCIA-CANOVAS F., RODRIGUEZ-LOPEZ, J.N. (2009): Generation of hydrogen peroxide in the melanin biosynthesis pathway, Biochimica et Biophysica Acta (BBA) **1794**, 1017-1029

PFEIFER, G.P., YOU, Y.H., BESARATINIA, A. (2005): Mutations induced by ultraviolet light, Mutation research **571**, 19-31

POLLOCK, P.M., HARPER, U.L., HANSEN, K.S., YUDT, L.M., STARK, M.,M ROBBINS, C.M., HOSTETTER, G., WAGNER, U., KAKAREKA, J., SALEM, G., POHIDA, T., HEENAN, P., DURAY, P., KALLIONIEMI, O., HAYWARD, N.K., TRENT, J., MELTZER, P.S. (2003): High frequency of BRAF mutations in nevi, Nat. Genet. **33**, 19-20

QUAN, T., HE, T., KANG, S., VOORHEESm J.J., FISHER, G.J. (2004): Solar ultraviolet irradiation reduces collagen in photodamaged human skin by blocking transforming growth factor b type II receptor/Smad signaling, American Journal of Pathology **165**, 741-751

REES, J.l. (2000): The Melanocortin 1 Receptor (MC1R): More Than Just Red Hair, Pigment Cell Research **13**, 135–140

ROCHETTE, J.P., THERRIEN, J.P, DROUIN,R., PERDIZ, D., BASTIEN,N., DROBETSKY,E.A, EVELYNE Sage, E. (2003):UVA-induced cyclobutane pyrimidine dimers form predominantly at thymine–thymine dipyrimidines and correlate with the mutation spectrum in rodent cells, Nucl. Acids Res. **31**, 2786-2794

SAGRIPANTI, S., and KRAEMER, K. (1989): Site-specific Oxidative DNA Damage at Polyguanosines Produced by Copper Plus Hydrogen Peroxide, The Journal of biological chemistry **264**, 1729-1734

SATHYANARAYANA, U.G., MOORE, A. Y., LI, L., PADAR, A., MAJMUDAR K., STASTNY, V., MARKARLA P., SUZUKI, M., MINNA, J.D., FENG, Z., GASDAR, A.F. (2007): Sun exposure related methylation in malignant and non-malignant skin lesions, Cancer letters **245**, 112-120

SETLOW, R.B (1974): The wavelengths in sunlight effective in producing skin cancer,: a theoretical analysis, Proc. Natl Acad. Sci USA **71**, 3363, 3366

SIMON, J.D., PELES, D., WAKAMATSU, K., ITO, S. (2009): Current challenges in understanding melanogenesis: bridging chemistry, biological control, morphology,and function, Pigment Cell Melanoma Res. **22**; 563–579

Surveillance, Epidemiology, and End Results (SEER) (2002): http://seer.cancer.gov/

TAKEUCHI, S., ZHANG, W., WAKAMATSU, K., ITO, S., HEARING, V.J., KRAEMER, K.H., BRASH, D.E. (2004): Melanin acts as a potent UVB photosensitizer to cause an atypical mode of cell death in murine skin, PNAS **101**, 15076-81

THOMAS, N. E., KRICKER, A., FROM, L., BUSAM, K., MILLIKAN, R. C., RITCHEY, M. E., ARMSTRONG, B. K., LEE-TAYLOR, J., MARRETT, L. D., ANTON-CULVER, H., ZANETTI, R., ROSSO, S., GALLAGHER, R. P., DWYER, T., GOUMAS, C., KANETSKY, P. A., BEGG, C. B., ORLOW, I., WILCOX, H., PAINE, S., BERWICK, M., MUJUMDAR, U., HUMMER, A. J., MITRA, N., ROY, P., CANCHOLA, R., CLAS, B., COTIGNOLA, J., MONROE, Y., LITCHFIELD, M., TUCKER, P., STEPHENS, N., SWITZER, T., THEIS, E., CHOWDHURY, N., VANASSE, L., PURDUE, M., NORTHRUP, D., SACERDOTE, C., LEIGHTON, N., GILDEA, M., GRUBER, S. B., BONNER, J., JETER, J., KLOTZ, J., WEISS, H., MATTINGLY, D., PLAYER, J., TSE, C. K., REBBECK, T. R., KANETSKY, P., WALKER, A., PANOSSIAN, S., MOHRENWEISER, H., SETLOW, R., TAYLOR, J. L., MADRONICH, S.(2010): Associations of cumulative sun exposure and phenotypic characteristics with histologic solar elastosis. Cancer Epidemiol Biomarkers Prev.**19**, 2932-41

ULLRICH, S. E. (1994): Mechanism involved in the systemic suppression of antigen-presenting cell function by UV irradiation: keratinocyte-derived IL-10 modulates antigen-presenting cell function of splenic adherent cells, J. Immunol.**152**, 3410

URBACH, F. (1993): Environmental risk factors for skin cancer - recent results, Skin Cancer Res **128**, 243-262

WENCZL, E., VAN DER SCHANS, G.P., ROZA, L., KOLB, R.M., TIMMERMAN, A.j., SMIT, N.P., PAYEL, S., SCHOTHORST, A.A. (1998): Pheomelanin photosensitizes

UVA induced DNA damage in cultures human melanocytes, Journal Invest Dermto. **111**, 678-682

WOLFF, D. (1931): Melanin in the inner ear, Arch Otolaryngol. **14**, 195-211

World Health Orangisation (WHO) (2011): http://www.who.int/cancer/en/

YAMAGUCHI, Y., TAKAHASHI, K., ZMUDZKA, B.Z., KORNHAUSER, A., MILLER, S.A., TADOKORO, T., BERENS, W., BEER, J.Z., HEARING, V.J. (2006): Human skin responses to UV radiation: pigment in the upper epidermis protects against DNA damage in the lower epidermis and facilitates apoptosis, FASEB J. **20**, 1486-14788

YOUNG ,A.R. (1998): The sunburn cell , Photodermatol. **4**, 127-34

YOUNG, A.R. (2006) Acute effects of UVR on human eyes and skin, Prog Biophys Mol Biol **92**, 80-85

ZHANG, X., ROSENSTEIN, B.S., WANG, Y., LEBWOHL, M., MITCHELL, D.M., WEI, H. (1997): Induction of 8-oxo-7,8-dihydro-2'-deoxyguanosine by ultraviolet radiation in calf thymus DNA and HeLa cells. Photochem Photobiol. **65**, 119-124

ZIEGLER, A., JONASON, A.S., LEFFELL, D.J. (1994): Sunburn and p53 in the onset of skin cancer, Nature **372**, 773–776